



RESEARCH

2009-19

MnROAD Cell 64 Pervious Concrete: Third Year Performance Report

MnROAD
Office of Materials

Take the steps... Research...Knowledge...Innovative Solutions!

Transportation Research

A green arrow graphic is positioned at the bottom right. It starts as a dashed line on the left, curves upwards and to the right, and then becomes a solid line pointing towards the text "Transportation Research". The word "Research" is written along the curve of the arrow.

Technical Report Documentation Page

1. Report No. MN/RC 2009-19	2.	3. Recipients Accession No.	
4. Title and Subtitle MnROAD Cell 64 Pervious Concrete: Third Year Performance Report		5. Report Date June 2009	6.
7. Author(s) Ryan J. Rohne and Bernard I. Izevbekhai		8. Performing Organization Report No.	
9. Performing Organization Name and Address Office of Materials and Road Research Minnesota Department of Transportation 1400 Gervais Avenue Maplewood Minnesota 55109		10. Project/Task/Work Unit No.	
		11. Contract (C) or Grant (G) No.	
12. Sponsoring Organization Name and Address Minnesota Department of Transportation 395 John Ireland Boulevard Mail Stop 330 St. Paul, Minnesota 55155		13. Type of Report and Period Covered Final Report	14. Sponsoring Agency Code
15. Supplementary Notes http://www.lrrb.org/PDF/200919.pdf			
16. Abstract (Limit: 250 words)			
<p>This report evaluates the third year performance of the pervious concrete test Cell 64 located in the parking lot/driveway on the south side of MnROAD's pole barn. In this report, a device and procedure to evaluate the drainability of pervious concrete and a threshold for clogging was developed. In addition, the condition of the test cell was determined by Schmidt hammer measurements and distress mapping using the Mn/DOT <i>Pavement Distress Identification Manual</i>. Watermark/thermocouple data was also recorded to measure freeze-thaw cycles. The number of freeze-thaw cycles at discrete depths in the pavement was then compared to impervious concrete test cells at MnROAD. The Mn/DOT and Cemstone petrographic reports on cores that had been taken 4.5 months after construction are also included, although they were outlined in previous reports.</p> <p>It was found that the pervious concrete of Cell 64 experienced less freeze-thaw cycles than impermeable concrete pavements of similar thickness. The main change in surface distress from the first year to the third year of service was the presence of a longitudinal crack that extended the entire cell length and raveling of the top layer of concrete. Initiating at the pole barn at a joint in the concrete curb, the crack could have propagated the length of Cell 64 due to Falling Weight Deflectometer (FWD), traffic, or thermal loading. Knowledge of pervious concrete will be greatly expanded with the study of newly constructed test cells. These cells are Cell 85, Portland Cement Concrete (PCC) pervious on sand and 89, PCC pervious on clay on the MnROAD Low Volume Road.</p>			
17. Document Analysis/Descriptors Cell 64, Pervious Concrete, Freeze-Thaw Cycles, Drainability, Thermodynamics		18. Availability Statement No restrictions. Document available from: National Technical Information Services, Springfield, Virginia 22161	
19. Security Class (this report) Unclassified	20. Security Class (this page) Unclassified	21. No. of Pages 64	22. Price

MnROAD Cell 64 Pervious Concrete: Third Year Performance Report

Final Report

Prepared by

Ryan J. Rohne
Bernard I. Izevbekhai

Office of Materials and Road Research
Minnesota Department of Transportation

June 2009

Published by

Minnesota Department of Transportation
Research Services Section
Transportation Bldg.
395 John Ireland Boulevard, Mail Stop 330
St. Paul, Minnesota 55155-1899

This report represents the results of research conducted by the authors and does not necessarily represent the views or policies of the Minnesota Department of Transportation. This report does not contain a standard or specified technique.

The authors and the Minnesota Department of Transportation do not endorse products or manufacturers. Trade or manufacturers' names appear herein solely because they are considered essential to this report.

ACKNOWLEDGEMENTS

We acknowledge the collaboration of the Minnesota Department of Transportation and the Aggregate Ready Mix Association of Minnesota (ARM of MN) which extended through the first-year evaluation period. We are particularly grateful to Fred Corrigan, executive director, and Dan Frentress, training coordinator of ARM.

We are also indebted to our Office Director Keith Shannon and Research Manager Maureen Jensen for fostering this and similar research initiatives. Our appreciation also goes to the MnROAD Operations team.

TABLE OF CONTENTS

The MnROAD Facility and Cell 64 Overview	1
Cell 64 Overview	3
Instrumentation	3
Petrographic Analysis.....	5
Performance Evaluation.....	6
Distress Mapping	6
Schmidt Hammer Testing	8
Drainability Monitoring (Clogging).....	11
Freeze-Thaw Cycles	17
Conclusion	23
References.....	24

APPENDIX A: MnROAD Test Sections

APPENDIX B: Mn/DOT Petrographic Analysis Report

APPENDIX C: Cemstone Petrographic Analysis Report

APPENDIX D: Photos of Cell 64

LIST OF TABLES

TABLE 1: Drainability Measurements	14
TABLE B-1: Air Void System Analysis Results per ASTM C457 Linear Traverse	B-4

LIST OF FIGURES

FIGURE 1: MnROAD Mainline, Low Volume Road (LVR), and Cell 64.....	1
FIGURE 2: The MnROAD pole barn and location of Cell 64.	2
FIGURE 3: Cell 64 sensor tree (profile view, not to scale).....	4
FIGURE 4: Crack mapping and distress survey conducted on April 2, 2009.	7
FIGURE 5: Schmidt hammer measurements on July 11, 2008.....	9
FIGURE 6: Schmidt hammer measurements on April 2, 2009.	10
FIGURE 7: In-situ drainability measurement device.	13
FIGURE 8: Drainability measurement locations.....	15
FIGURE 9: Cell 64 on January 23, 2009.....	16
FIGURE 10: Freeze-thaw cycles measured by watermarks in pavement, base, and subgrade.	18
FIGURE 11: Comparison of number of freeze-thaw cycles calculated using different definitions at various depths below Cell 64.....	19
FIGURE 12: Number of freezing cycles at various depths below pervious and impervious PCC pavements of similar thickness.....	20
FIGURE 13: Temperature 36 in. below pavement surface.....	21
FIGURE 14: Mid-depth temperature in pervious (PPCC) and impervious (PCC) test cells at MnROAD.....	22
FIGURE A-1: MnROAD Phase I Mainline test sections.	A-1
FIGURE A-2: MnROAD Phase II Mainline test sections.	A-2
FIGURE A-3: MnROAD Phase I Low Volume Road (LVR) test sections.	A-3
FIGURE A-4: MnROAD Phase II Low Volume Road (LVR) test sections.	A-4
FIGURE B-1: Schematic and photo showing the layout of the pervious concrete at MnRoad.....	B-3
FIGURE B-2: Illustration of how cores are sectioned for microscopic evaluation.	B-4
FIGURE B-3: Arrows point to fine cracks in paste in core 2.....	B-5
FIGURE B-4: Microscopic view of polished slabs from core 3 showing several fine tight cracks.	B-6
FIGURE D-1: Tooled joint, Top: 9.21.06, Bottom: 8.11.08.	D-1
FIGURE D-2: Header/construction joint, Top: 9.21.06, Bottom: 8.11.08.	D-2
FIGURE D-3: Mix #2 surface raveling, Top: 01.04.06, Bottom: 8.11.08.....	D-3
FIGURE D-4: Coterminous joint at Mixes #2 and #3, Top: 9.21.06, Bottom: 8.11.08.	D-4
FIGURE D-5: Header/construction joint, facing south, 8.11.08.	D-5
FIGURE D-6: Tooled joint, 4.02.09.	D-5
FIGURE D-7: Area of severe raveling in Mix 2, 4.02.09.....	D-6
FIGURE D-8: Raveled surface material in Mix 2, 4.02.09.	D-6

EXECUTIVE SUMMARY

This report evaluates the first three years performance of the pervious concrete test Cell 64 located in the parking lot/driveway on the south side of MnROAD's pole barn. In this report, a device and procedure to evaluate the drainability of pervious concrete and a threshold for clogging was developed. In addition, the condition of the test cell was determined by Schmidt hammer measurements and distress mapping using the Mn/DOT Pavement Distress Identification Manual. Watermark/thermocouple data was also recorded to measure freeze-thaw cycles. The number of freeze-thaw cycles at discrete depths in the pavement, base, and subgrade was then compared to impervious concrete test cells at MnROAD. The Mn/DOT and Cemstone petrographic reports on cores taken 4.5 months after construction are also included.

The main change in surface distress from the first year to the third year of service was the presence of a longitudinal crack that extended the length of Cell 64. Initiating at the pole barn at a joint in the concrete curb, it could have propagated the length of Cell 64 due to Falling Weight Deflectometer (FWD), traffic, or thermal loading. After the winter of 2008/09, there was severe raveling of the surface layer in parts of Mix #2.

To measure seasonal variations in permeability and also to prevent destroying the test cell by taking concrete cores, an in-field permeability measurement device was developed. This device uses a time function for emptying under a varying head. An inverted Humboldt H-4245 sand cone was modified and used to measure changes in the hydraulic conductivity. A threshold of 5 minutes was used to determine clogging. Measurements made before and after Cell 64 was swept indicate that sweeping decreased hydraulic conductivity and can cause clogging. Further changes in hydraulic conductivity will be monitored seasonally and after significant rainfall or maintenance events.

Freeze-thaw cycles were monitored by analyzing the data from two sensor trees of watermarks and thermocouples within the pavement and subgrade. The number of freeze-thaw cycles at different depths in the pavement, base, and subgrade were compared between Cell 64 and other concrete pavements of similar thickness at MnROAD. It was found that the pervious concrete of Cell 64 experienced less freeze-thaw cycles than impervious pavements of similar thickness.

Changes in hydraulic conductivity, surface distress, and strength (Schmidt hammer) will continue to be monitored. Knowledge of pervious concrete will greatly be expanded with the testing of Cells 85, PCC pervious on sand and 89, PCC pervious on clay on the MnROAD Low Volume Road.

THE MNROAD FACILITY AND CELL 64 OVERVIEW

The Minnesota Department of Transportation (Mn/DOT) initially constructed the Minnesota Road Research Project (MnROAD) between 1990 and 1994. MnROAD is located along Interstate 94, approximately forty miles northwest of Minneapolis/St. Paul and is an extensive pavement research facility consisting of two separate roadway segments containing 51 distinct test cells as shown in Figure 1. Each MnROAD test cell is approximately 500 feet long. Subgrade, aggregate base, and surface materials, as well as roadbed structure and drainage methods vary from cell to cell. All data presented herein, as well as historical sampling, testing, and construction information, can be found in the MnROAD database and in various publications. Layout and designs used for the Mainline and Low Volume Road are included in Appendix A.



FIGURE 1: MnROAD Mainline, Low Volume Road (LVR), and Cell 64.

Although not part of the MnROAD Mainline or Low Volume Road (LVR), Cell 64 is a part of the overall MnROAD facility. Cell 64 is located on the south side of the MnROAD pole barn as part of a bituminous parking lot, as shown in Figure 2. A 64-ft by 20-ft section of the bituminous driveway was removed in order to place the drainage system, base, pervious concrete, and concrete curb surrounding the pervious concrete slab. The actual size of the pervious concrete portion of the driveway is 60-ft by 16-ft, surrounded by a 2-ft concrete curb on all sides.

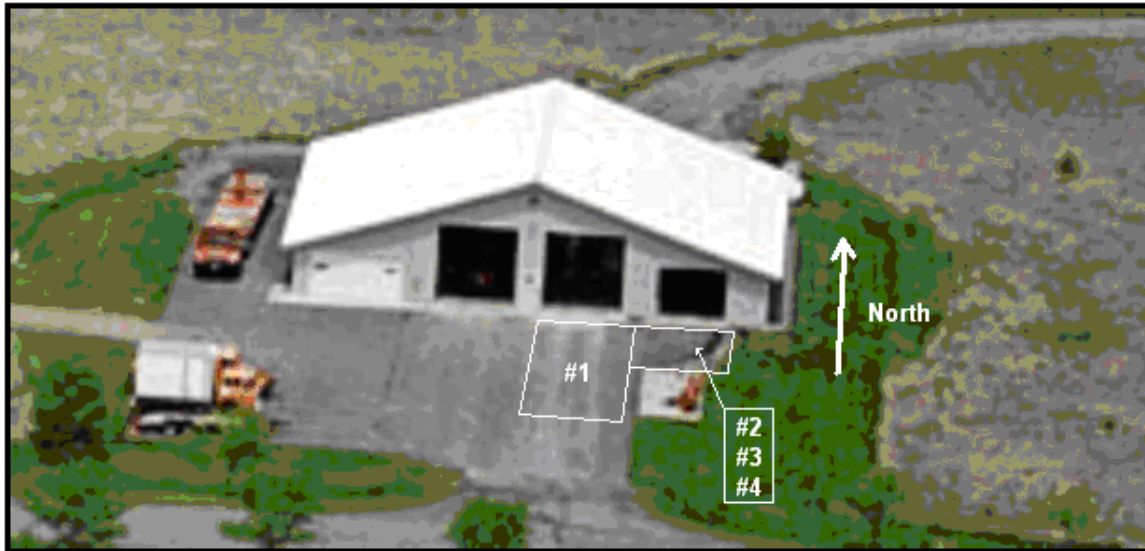


FIGURE 2: The MnROAD pole barn and location of Cell 64.

- Area #1 – Cell-64 pervious concrete driveway (60' by 16').
- Area #2 – Pervious practice placement (Mix #3).
- Area #3 – Regular concrete placed between Area #2 and Area #4.
- Area #4 – Pervious practice placement (Mix #4).

The MnROAD mainline consists of a 3.5-mile 2-lane interstate roadway carrying “live” traffic. The Mainline consists of 5-year and 10-year pavement designs as well as whitetopping test sections. Originally, a total of 23 cells were constructed consisting of 14 HMA cells and 9 Portland Cement Concrete (PCC) test cells.

Parallel and adjacent to Interstate 94 and the Mainline is the Low Volume Road (LVR). The LVR is a 2-lane, 2½-mile closed loop that contains 20 test cells. Traffic on the LVR is restricted to a MnROAD operated vehicle, which is an 18-wheel, 5-axle, tractor/trailer with two different loading configurations. The "heavy" load configuration results in a gross vehicle weight of 102 kips (102K configuration). The “legal” load configuration has a gross vehicle weight of 80 kips (80K configuration). On Wednesdays, the tractor/trailer operates in the 102K configuration and

travels in the outside lane of the LVR loop. The tractor/trailer travels on the inside lane of the LVR loop in the 80K configuration on all other weekdays. This results in a similar number of ESALs being delivered to both lanes. ESALs on the LVR are determined by the number of laps (80 per day on average) for each day and are entered into the MnROAD database.

Currently, the MnROAD research facility is under Phase II reconstruction. Phase two encompasses more than 20 research projects and reconstruction of 35 cells. Construction began in 2007 and will be completed in 2009. The new Phase II Mainline and new Phase II Low Volume Road (LVR) cell design/layout can be found in Appendix A. After Phase II construction has been completed on the LVR in the winter of 2008/2009, the MnROAD semi will only operate at the 80K “legal” configuration and only drive on the inside lane. The outside lane will only experience environmental loading.

Cell 64 Overview

The Cell 64 pervious concrete driveway was constructed in late September of 2005 in a partnership agreement with Mn/DOT and the Aggregate Ready Mix Association of Minnesota (ARM of MN) [1]. The intent of this partnership agreement was to construct a pervious concrete of similar thickness to concrete pavements of typical transportation uses and monitor the response to weather and loading. The Cell 64 concrete driveway was placed in one day over the course of approximately 4.5 hours. It took six loads of concrete from six different trucks to complete the driveway slab. Placing pervious concrete is slower than placing traditional non-pervious concrete, so small loads were used in each concrete truck so the loads would not get old during placing.

Three mix designs were used for the concrete driveway, with the aggregate being the major component varied between them. Fly ash content, cement content, and water content varied slightly for each mix design, but the water/cement ratio and volume of admixtures remained the same between the three mix designs. Mix #1 contained a 3/8 in. dolomite (Mn/DOT 3137/CA-80, Source 80 171041) for the first 25.5 ft from the pole barn. Mix #2 contained both the 3/8 in. dolomite aggregate in addition to a rounded gravel of maximum nominal size 3/8 in. (Mn/DOT 3137 – Aggregate Industries) for the next 22 ft from the pole barn. Mix #3, placed in the final 12.5 ft of the driveway, contained a dolomite gravel of maximum nominal size ½ in. (Mn/DOT 3137/CA-80, Source 70 182001). Mix #4 was designated to the concrete placed in Area #4 in Figure 2. The pervious concrete placed in this area consisted of Mix #1 contaminated with sand from the mixer.

Instrumentation

Vibrating wire strain gauges, dynamic strain gauges, thermocouples, and watermarks were embedded in Cell 64 during construction. Two sensor trees of thermocouples and water blocks were installed to an approximate depth of four feet below the surface of the driveway to monitor the temperature profile and frost depth within the pervious concrete, base material, and subgrade. Thermocouples and water blocks were placed at discrete locations on the sensor tree according to Figure 3. The sensor trees were placed two feet east of the driveway centerline, at 15 ft and 45 ft north of the southernmost edge of the pervious concrete driveway in Mixes #3 and #1

respectively. More information on the sensor installation can be found in the first year performance report [2].

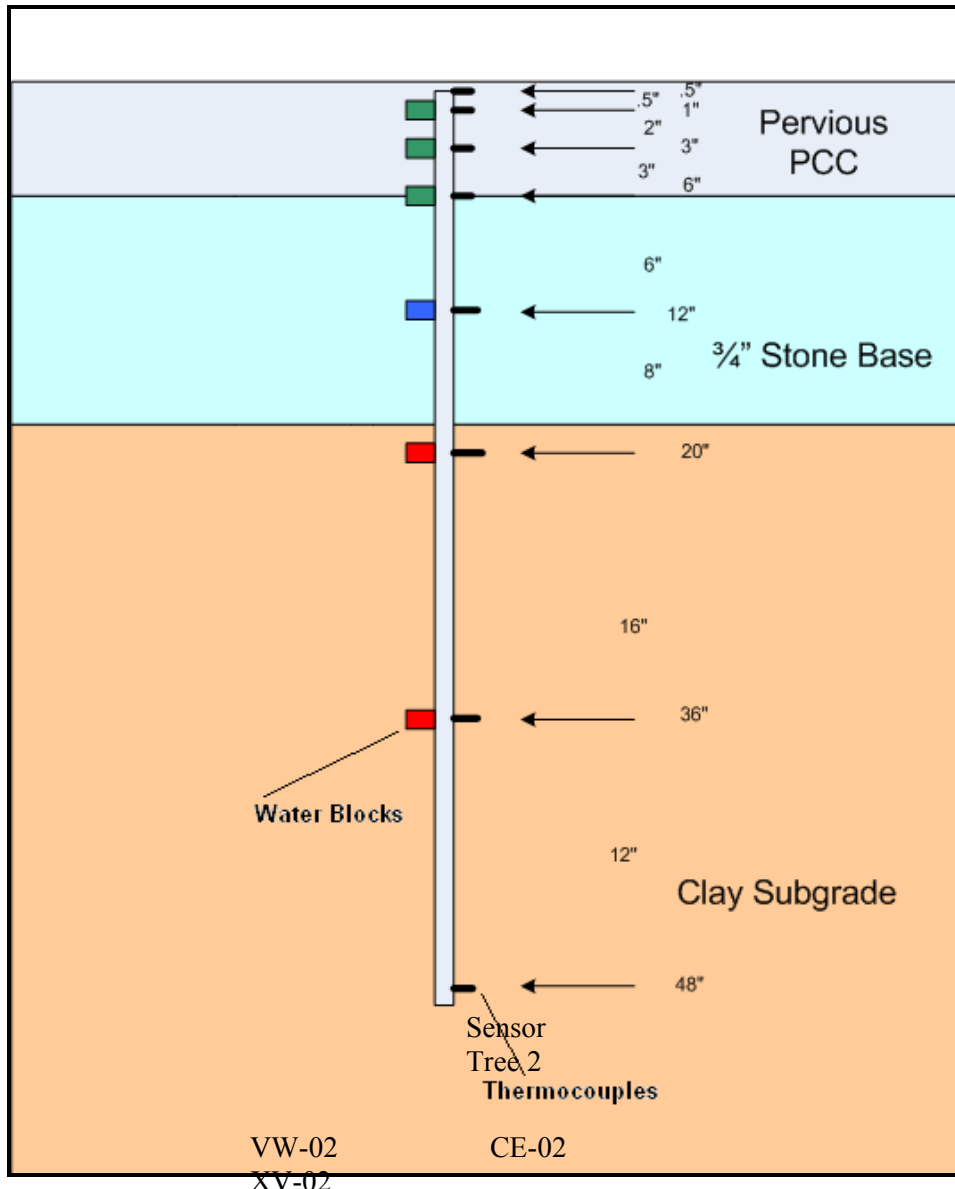


FIGURE 3: Cell 64 sensor tree (profile view, not to scale).

PETROGRAPHIC ANALYSIS

The previous chapter presented a general overview of the MnROAD test facility and test Cell 64. This chapter summarizes the results of Mn/DOT's and Cemstone's petrographic analysis on cores taken after approximately four months of service. The Mn/DOT petrographic report is included in Appendix B and Cemstone's petrographic report is included in Appendix C. A more detailed discussion can be found in the first year performance report [2] although the full petrographic reports are only included in this report.

The cores taken by Mn/DOT represent mix designs #3 and #4. ASTM C 457 Linear Traverse was performed on both cores to quantify the various elements of the pervious concrete. Both mixes contained traces of sand that were not specified in the mix design. The presence of the sand may have resulted from contamination left in the mixer barrel from previous concrete pours. Air content of the pervious concrete consisted of $\leq 1\%$ entrained air, and the spacing factor was much lower than recommended for freeze-thaw resistance in normal Portland Cement Concrete. Both cores had a higher air void percentage near the bottom. Fine, tight cracks were evident in both cores at all depths. The core from Mix #3 displayed these cracks through the paste running from air void-to-air void, air void-to-aggregate, aggregate-to-aggregate, and occasionally following the aggregate-paste interface (Interfacial Transition Zone). The core from Mix #4 displayed these cracks as well, although they were more apparent near the top of the core than in Mix #3. In addition, cracks in the core from Mix #4 ran through the aggregate as well as the paste. It is difficult to determine the cause of these cracks, but some possibilities include: 1) exposure to repeated freeze-thaw cycles, 2) incomplete hydration from low water/cement ratio, 3) exposure of the pervious driveway to heavy loads.

Cemstone provided petrographic analysis of four cores taken from the pervious driveway in accordance with ASTM C 856 Petrographic Examination of Hardened Concrete and ASTM C 457 Linear Traverse. The cores represent the material near the south end of the driveway where raveling of the top layer has occurred and the northern part of the driveway that exhibits little to no raveling.

Cemstone's analysis determined that the water/cement ratio was relatively low (approximately 0.30 to 0.40) based on the optical and physical properties of the cementitious paste. In addition to this, all four core-samples showed paste fraction inhomogeneities of lower water/cement ratio paste within pockets of high water/cement ratio paste, especially within the recesses of the coarse aggregate particles. Moderate microcracking, and subsequent carbonation of those cracks, was common in the top 3 in. of the cores. The top $\frac{1}{4}$ in. to $\frac{1}{2}$ in. of the cores exhibited extensive microcracking consistent with severe shrinkage. The air void system in these cores consisted mainly of compaction voids that ranged from 21% to 31%.

PERFORMANCE EVALUATION

The previous chapter summarized the results of petrographic analysis on cores taken after four months of service. In this chapter, Schmidt hammer and hydraulic conductivity tests and changes in surface distress between one and three years of service are discussed.

Distress Mapping

On September 9, 2006, August 11, 2008, and again on April 2, 2009 the overall surface condition of Cell 64 was surveyed using Mn/DOT's Pavement Distress Identification Manual as a guide. The methods described in the manual are typically utilized for much larger stretches of roadway. However, the manual provides a standardized method as well as a terminology familiar to most transportation and pavement engineers.

The main change in surface condition from the 2006 to the 2008 survey was the presence of a longitudinal crack running the length of the test cell. The crack appeared to have propagated from the joints in the concrete curb that runs between the pole barn and the pervious test cell. This crack could have propagated the length of the slab due to FWD testing, traffic loading, or thermal movement. Also, after the winter of 2008/09, severe surface raveling was observed in portions of Mix #2. This raveling occurred in the same location as the raveling that was observed shortly after construction.

On the August 11, 2008 condition survey, Mix #1 showed moderate spalling at the tooled joint and raveling at the joint where Mixes #1 and Mixes #2 are co-terminus. Mix #2 showed moderate to severe raveling on the surface of the concrete, with moderate to severe raveling and spall at the joints. Mix #3 showed low raveling on the surface with moderate to severe raveling and spall at the joints.

During the winter of 2008/09 significant changes in distress occurred in Cell 64. The top layer of pervious concrete along the tooled joint in Mix #1 as well as significant portions of Mix #2 showed sever raveling. The affected area in Mix #2 is the same area that experienced surface raveling shortly after construction [2]. The locations of cracks in Cell 64 and the areas of raveling are shown in Figure 4.

After three years, Mix #1 shows the least surface raveling/spall with Mix #2 having the most. Most of the raveling/spall in Mix #2 occurred shortly after placement and then again in the spring of 2009. As shown in Appendix D, the top $\frac{1}{4}$ to $\frac{1}{2}$ in. of concrete in some areas of Mix #2 raveled away shortly after placement and again in spring 2009. The original raveling that occurred just after construction likely occurred because the mix became too dry by not being covered with plastic early enough or by over finishing the surface. The raveling that began in spring 2009 likely occurred because the pavement was clogged. Water or snow could have been trapped in the pervious concrete. Then when it froze or was compacted into ice, the expansive pressure could have deteriorated the paste around the top layer of aggregate, resulting in raveling of this layer.

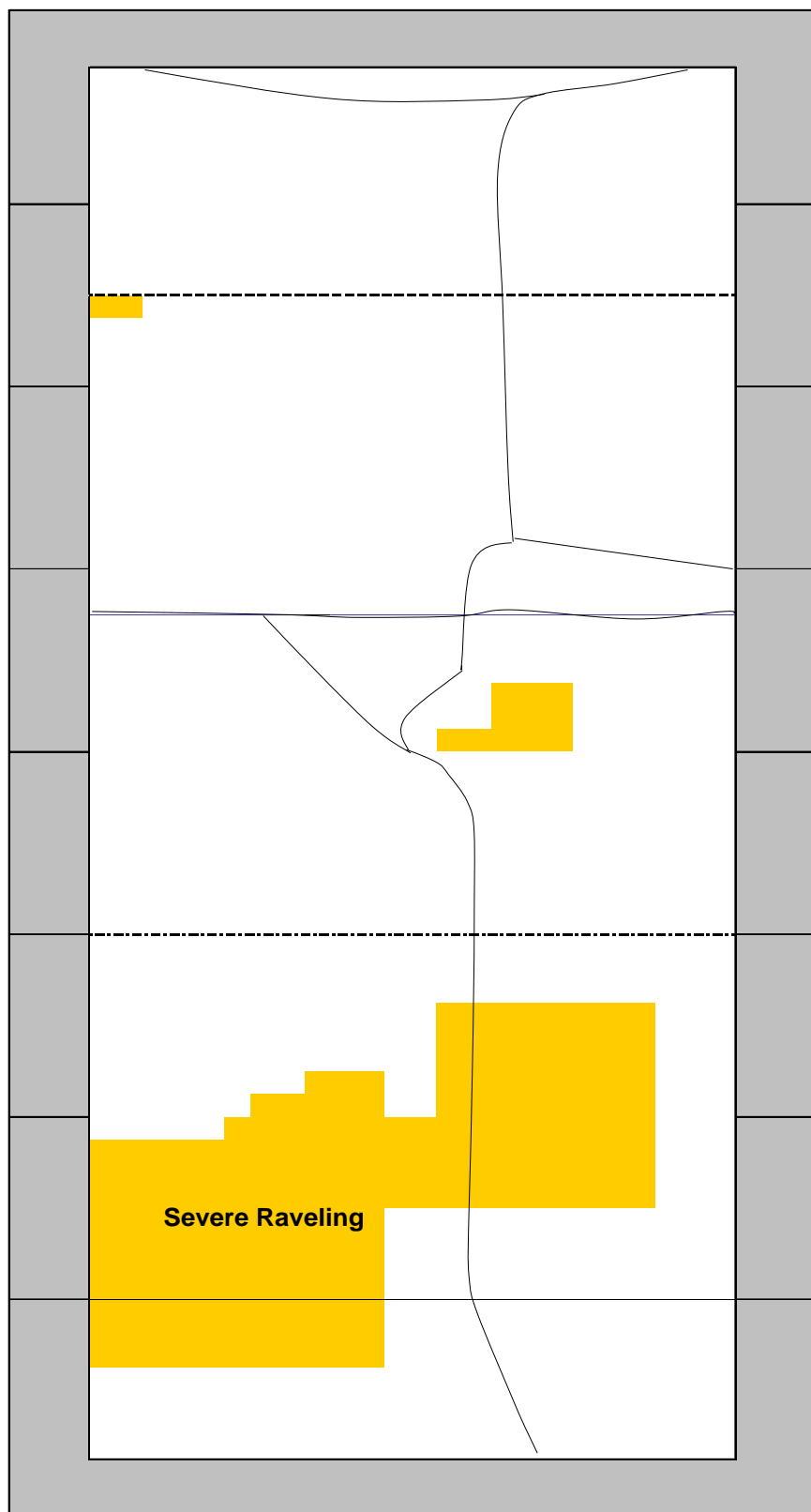


FIGURE 4: Crack mapping and distress survey conducted on April 2, 2009.

Schmidt Hammer Testing

The Proceq digi-schmidt digital Schmidt hammer was used to measure differences in concrete surface strength on July 11, 2008 and again on April 2, 2009. Measurements were taken every two feet, starting and ending at the concrete curb, in the east-west direction and every ten feet in the north-south direction. The test locations and measured values are shown in Figure 4 for the 2008 testing and Figure 5 for the 2009 testing. The compressive strength was calculated from the rebound number using the Proceq digi-Schmidt built in conversion equations. The equation used was the Average Curve J. This curve is the average of three curves developed in Japan; early strength J, blast furnace J, and Portland cement J [3]. This curve was used because none of the other curves were appropriate. The shape coefficient used was for 6x12 in. cylinders.

Schmidt hammer measurements on pervious concrete are much more difficult than in normal PCC because the surface is discontinuous in pervious concrete and it is difficult to make good contact between the Schmidt hammer and the concrete surface. For the procedure used in this report, measurements were made where the paste or aggregates were smooth enough to make good contact.

The values in Figures 4 and 5 are the average of three measurements at each location. In 2008, the Schmidt hammer results varied from 1223 psi to 5977 psi in the pervious concrete and 3968 psi to 6792 psi in the concrete curb. Mix #1 had the lowest compressive strength values while the raveled portion of Mix #2 had the highest. Because of the high strength of Mix #2, the top layer most likely raveled due to over working or drying. If Mix #2 raveled due to low strength, it would be expected that the Schmidt readings in the raveled areas would indicate low strength, but the opposite is true, the highest strengths were measured in the raveled areas. The lowest Schmidt hammer values measured were for Mix #1, where the surface distress was also the lowest.

The results of the 2009 testing were similar to the 2008 testing. Mix #1 had the lower strength than Mix #2. Measurements were not made on the south end of the test cell because of loose material in that area due to surface raveling. As evident in Figures 4 and 5, there is great variability in the measured Schmidt hammer values. This is likely due to the uneven surface of the pervious concrete.

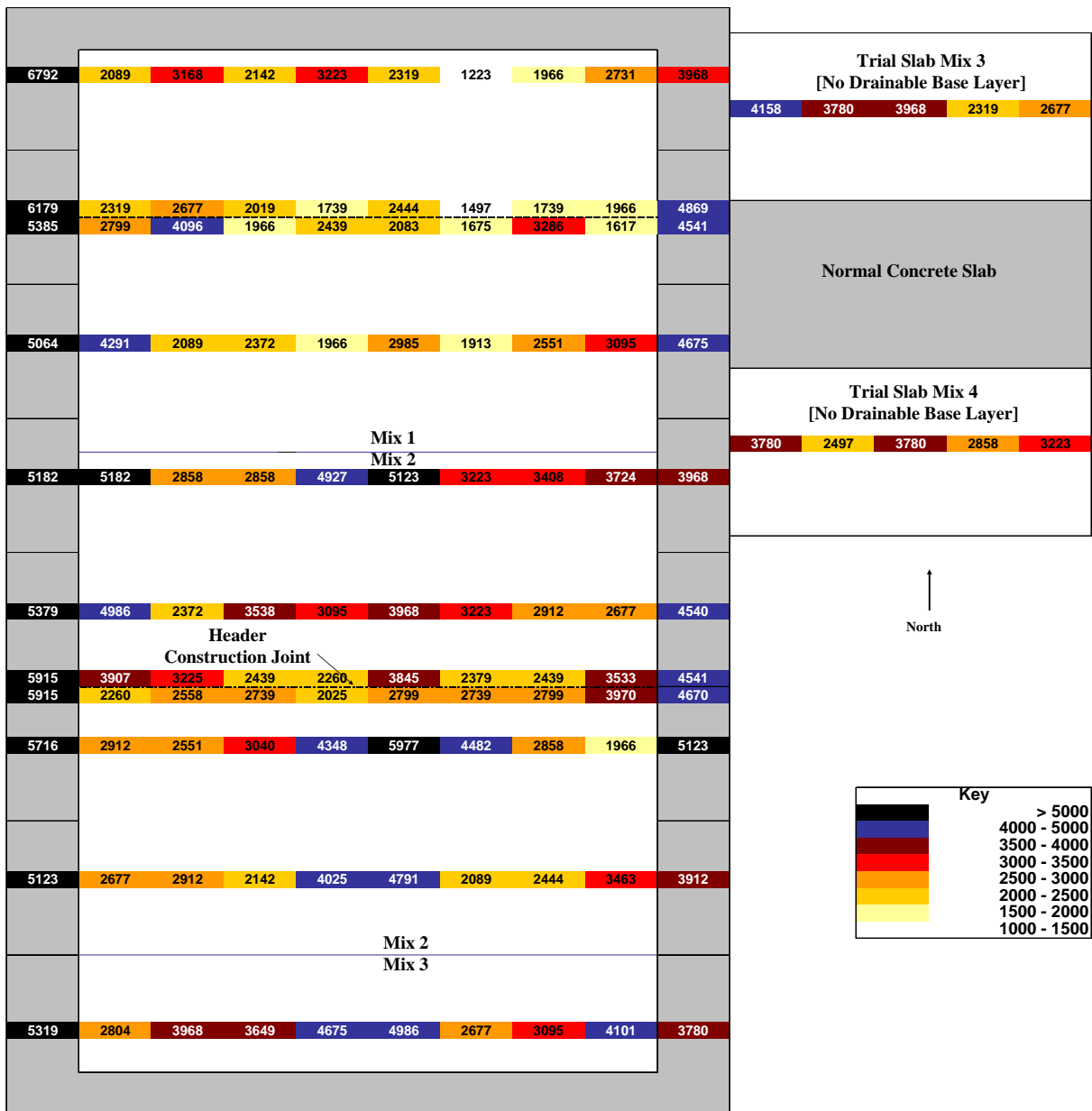


FIGURE 5: Schmidt hammer measurements on July 11, 2008.

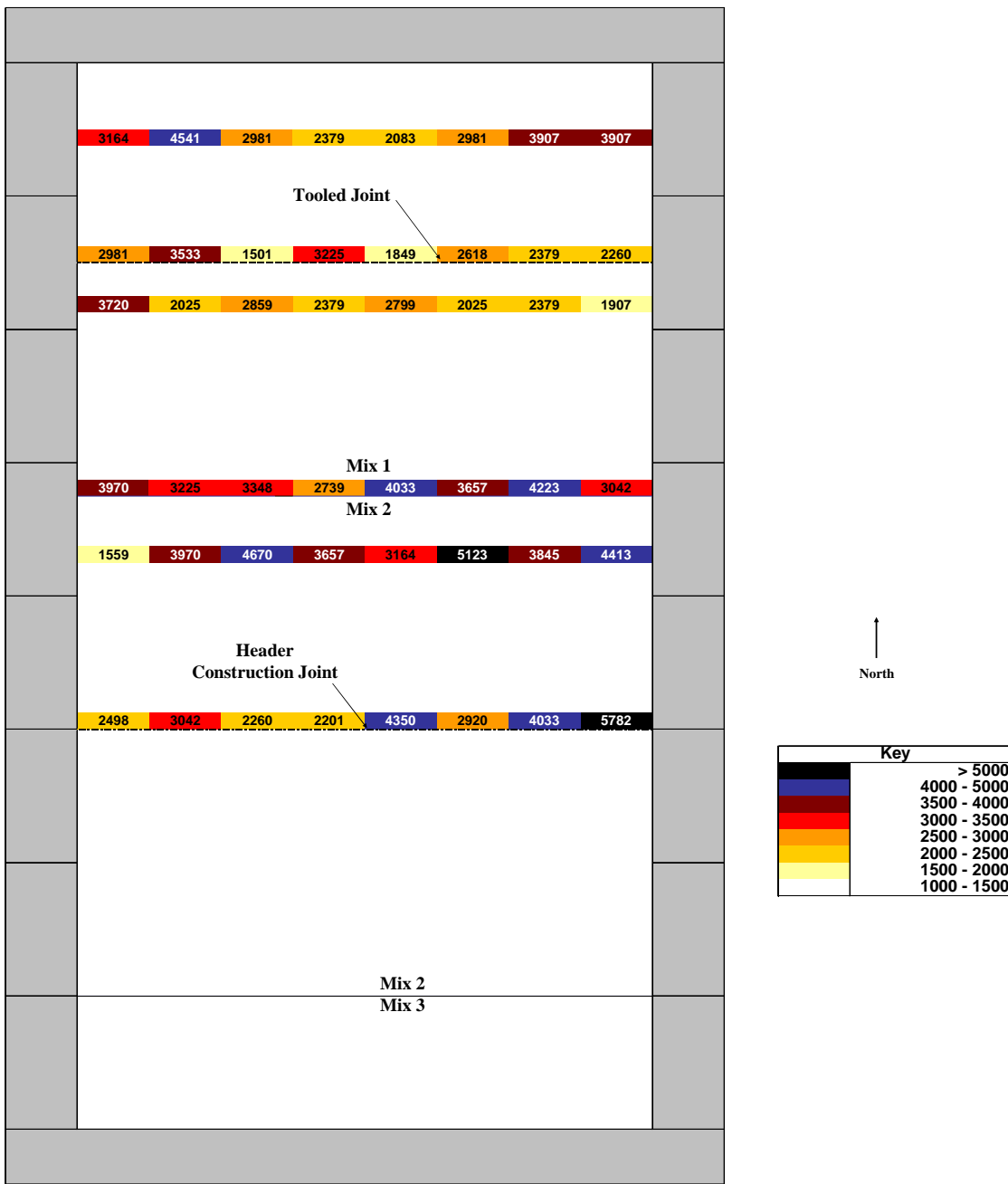


FIGURE 6: Schmidt hammer measurements on April 2, 2009.

Drainability Monitoring (Clogging)

In order to measure the performance of the pervious concrete, a way in which to measure changes in flow properties due to winter sanding/salting, plowing, and sweeping is needed to insure that the pervious concrete remains unclogged. Traditional methods for monitoring hydraulic conductivity of pervious concrete involved removing cores and testing them using either continuous or falling head permeability tests [4-6]. To measure seasonal variations in flow properties and also to prevent destroying the test cell by taking concrete cores, an in-field permeability measurement device was required. Our experiment performed in-situ uses a time function for emptying under a varying head.

The device developed was an inverted Humboldt H-4245 sand cone as shown in Figure 7. Duct seal compound was used to create a seal between the pervious concrete and the bottom cone flanged opening. The drainability was measured by recording the time it took for water to drop between two lines along the straight portion of the 1-gal plastic jar. The drainability test points for Cell 64 are shown in Figure 8. Measurements will periodically be repeated at these same locations to determine changes in permeability.

The permeability was determined as follows. From continuity, the flow rate of the water in the plastic jar must equal the flow rate exiting the sand cone, Equation 1.

$$\frac{\pi d^2}{4} dh = v_0 A_0 dt \quad (1)$$

Then Bernoulli gives Equation 2.

$$\frac{P_1}{\rho_1 g} + \frac{v_1^2}{2g} + z_1 + \text{losses} = \frac{P_2}{\rho_2 g} + \frac{v_2^2}{2g} + z_2 \quad (2a)$$

$$v_0 = \lambda \sqrt{2gh} \quad (2b)$$

Where λ is a constant that accounts for piezometric head loss due to the sand cone device. Combining equations 1 and 2, reorganizing, and integrating both sides gives:

$$-\frac{\pi d^2 \sqrt{h}}{2\lambda \sqrt{2g} A_0} + C = T \quad (3)$$

Then substituting the boundary conditions of $h = H$ when $T = 0$ gives:

$$-\frac{\pi d^2}{2\lambda \sqrt{2g} A_0} (\sqrt{h} - \sqrt{H}) = T \quad (4)$$

Equation 4 is different than the equation typically used for falling head permeability because in porous concrete, the term containing the velocity head cannot be neglected, which is typically done in soils. To compensate for the losses due to the reduction in cross-sectional area at the valve, the time it takes for the perveameter to empty in air, $T_{air} = 10$ s, is introduced. When $T = 10$ s, $\lambda' = 1/\lambda = 1$, and the left side of Equation 4 must equal 10 s which gives:

$$\lambda' 10 = T \quad (5)$$

Equation 5 relates the hydraulic conductivity of the pervious concrete as a multiple of the time it takes for the perveameter to empty in air. Equation 5 is similar to:

$$Q = KiA \quad (6a)$$

$$V = KiAt \quad (6b)$$

Where Q is discharge, K is hydraulic conductivity, A is area, i is the hydraulic gradient, V is volume, and t is the time of discharge. Assuming a tortuous path around a rounded aggregate, the hydraulic gradient is equal to

$$i = \frac{2r}{r\pi} = 0.64 \quad (6c)$$

The effective porosity of the pavement system for a 7 in. thick pervious concrete with 20% porosity and 12 in. thick drainable base with 40% porosity is 33% therefore the effective volume available to store water is $V_{eff} = 0.33 \cdot 19 \cdot A$. Based on the apparatus used and the minimum time of discharge for good draining pavement, the discharge time for a 6 in. drop in head was 17 s which gives a hydraulic conductivity of $K = 0.35$ in/s. The effective time (t_{eff}) to fill the storage is given by:

$$t_{eff} = \frac{V_{eff}}{iKA} = \frac{0.33 \cdot 19 \cdot A}{0.64 \cdot 0.35 \text{ in/s} \cdot A} = 28s \quad (7)$$

Since the water in our test is not restricted to vertical flow and can flow horizontally as well, an equipment multiplier must be used to convert the effective hydraulic conductivity to one-dimensional flow. This conversion factor is obtained by diving the effective time to fill the storage (t_{eff}) to fill the storage by the minimum time measured in clean pervious concrete.

$$EM = \frac{t_{eff}}{t} = \frac{28s}{17s} = 1.65 \quad (8)$$

The effective time (t_{eff}) of discharge when the hydraulic conductivity is reduced to 10% of its initial clean value is 280 s. Then using the equipment multiplier (EM), the actual measured time using the developed perveameter is:

$$t_d = \frac{t_{eff}}{EM} = \frac{280s}{1.65} = 170s(2.8 \text{ min}) \quad (9)$$

This procedure suggests ≈ 3 min. as the threshold for clogging when clogging is defined as a reduction of 90% in hydraulic conductivity.

The measured hydraulic emptying times are shown in Table 1. The threshold for clogging used was 5 min. (300 s). Starting with the 8.04.08 measurement event, if the perveammeter did not empty in 300 s or less, the distance that the water dropped (in inches) from the starting point was measured to determine the severity of clogging.

Between the 7.11.08 and 8.04.08 measurement events, the test cell was swept. As shown in Table 1, measurement locations that were previously clogged remained clogged and locations that were not clogged either became clogged, or the emptying time increased. This shows that sweeping contributes to clogging of the pervious pavement.



FIGURE 7: In-situ drainability measurement device.

TABLE 1: Drainability Measurements

Date	Time (s)											
	L1	L2	L3	L4	L5	L6	R1	R2	R3	R4	R5	R6
6.26.08	CLG	318.2	CLG	CLG	181.9	121.4	-	-	-	-	-	-
7.11.08	CLG	CLG	-	-	CLG	-	-	-	-	60.0	313.0	-
8.04.08	1.5"	1.25"	1.5"	3.75"	2.25"	2.0"	166.4	164.4	3.0"	105.9	4.5"	285.8
10.31.08	2.0"	2.75"	2.25"	3.0"	3.5"	4.5"	4.5"	3.0"	3.25"	4.5"	4.25"	3.75"
3.14.09	1.75"	131	1.75"	102	42	3.25"	3.75"	250	2.0"	195	2.5"	2.0"

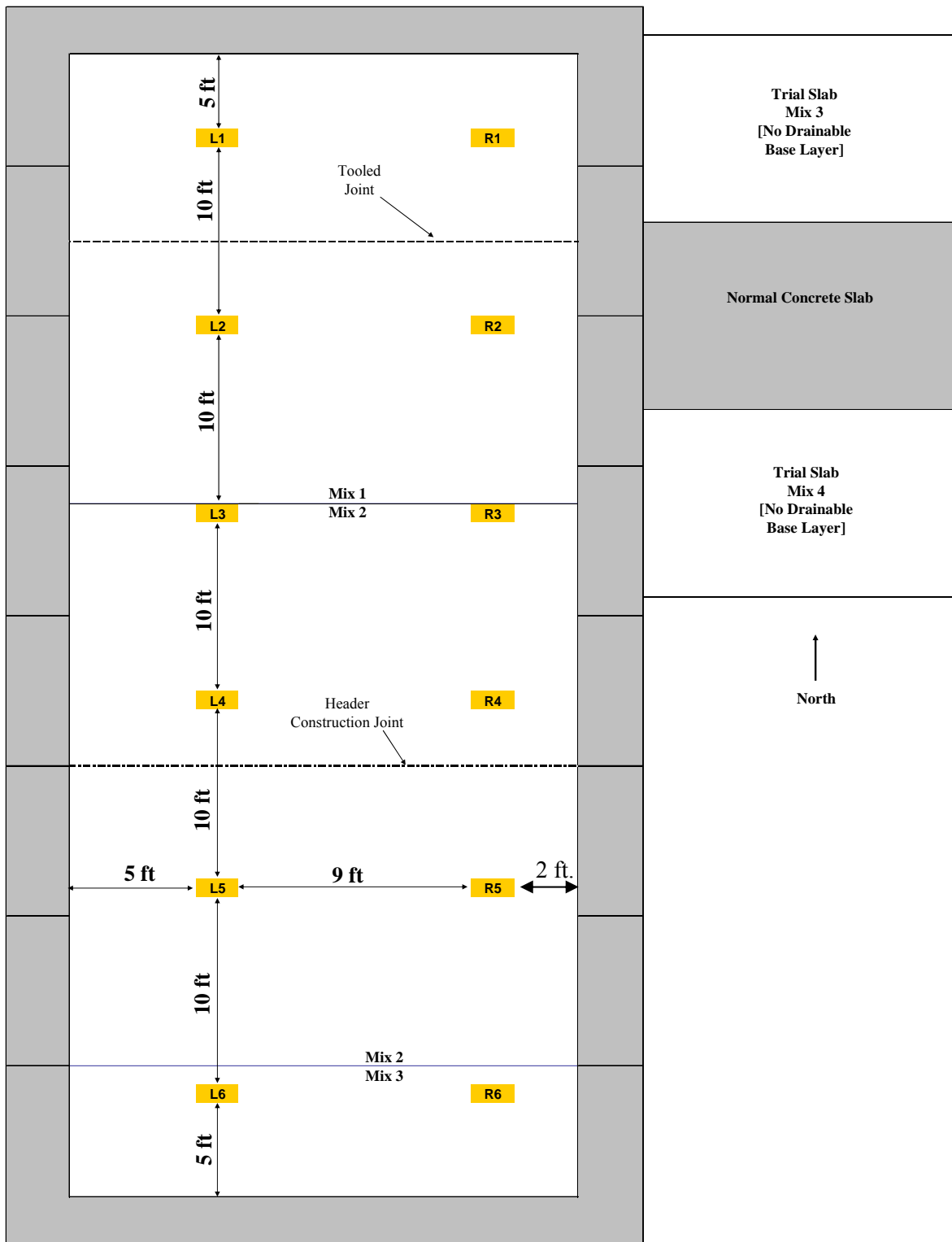


FIGURE 8: Drainability measurement locations.

Hydraulic conductivity measurements were attempted on January 26, 2009 to determine if water could still drain through the pavement when frozen. This situation could occur if the surface of the pavement thawed on a warm sunny day while the pavement further from the surface stayed frozen. The measurements were not able to be taken because the surface of the pervious concrete was covered with ice and snow as shown in Figure 9. The MnROAD operations staff noted that salting and plowing was not as effective in keeping the surface free of ice as in impermeable pavements. In the asphalt driveway surrounding Cell 64, the salt would melt the ice and form a salt solution which would then melt the ice in-between the salt grains. In the pervious concrete, this salt solution drained away through the pavement and did not effectively melt the ice at the surface. In the pervious HMA and concrete pavements of test Cell 85, 86, 88, and 89 this phenomena was not observed because salt had not been applied to the LVR. Seasonal measurements will continue to monitor changes in hydraulic conductivity.



FIGURE 9: Cell 64 on January 23, 2009.

FREEZE-THAW CYCLES

In a wet hard freeze climate such as Minnesota's, freeze-thaw durability will determine whether pervious pavements will gain wide spread usage. To effectively monitor a pavements ability to resist freeze-thaw degradation, first the number of freeze-thaw cycles that the pavement has experienced needs to be determined. In Cell 64, thermocouple and watermark trees were installed to accomplish this. Previous chapters described how Cell 64 performed under environmental loading. This chapter attempts to quantify the environmental loading by determining how many freeze-thaw cycles the pavement experienced. A comparison to standard PCC and HMA pavements of similar thickness is also made.

Two sensor trees of thermocouples and water blocks were installed to an approximate depth of four feet below the surface of the pervious concrete, base material, and subgrade. Thermocouples and water blocks were placed at discrete locations on the sensor tree according to Figure 3. The watermark/thermocouple trees were monitored to identify temperature trends in the soil/concrete profile, and freeze-thaw events. Since the watermark data indicates a change in phase from liquid to solid, it provides a better way in which to count freeze-thaw cycles than thermocouples which only indicate temperature.

Figure 10 shows the resistance read by the watermark sensors for six discrete depth intervals taken from November 24, 2005 to December 17, 2008 with the exception that data from May 5, 2006 until April 25, 2007 is missing. The white vertical lines in Figure 10 indicate the location of the discontinuity in the data. The resistance changes markedly when the sensor detects frost, and the graphs show several freeze thaw events that may have even reached to the CA-50 base material. During the winter of 2007/2008, freeze thaw events as deep as 36 in. below the pavement surface are shown.

In order to count the number of freeze-thaw cycles that the pavement experienced, a freeze-thaw cycle needs to be defined. The definition in the ASTM C 666 procedure for determining the freeze-thaw resistance of concrete works well in the laboratory setting but in the field air temperatures are erratic. Using a temperature fall and rise above 0 °C is not accurate because water in concrete cannot freeze or thaw instantaneously but needs a prolonged period of time to freeze or thaw depending on the temperature. Dissolved ionic solutions within the concrete can also have a lower freezing temperature than pure water. A better definition of a freeze-thaw cycle is needed. A procedure developed in early 2006 by the Mn/DOT research staff counted one freeze-thaw cycle every time the daily minimum temperature dropped below 0 °C and the daily maximum rose above 0 °C.

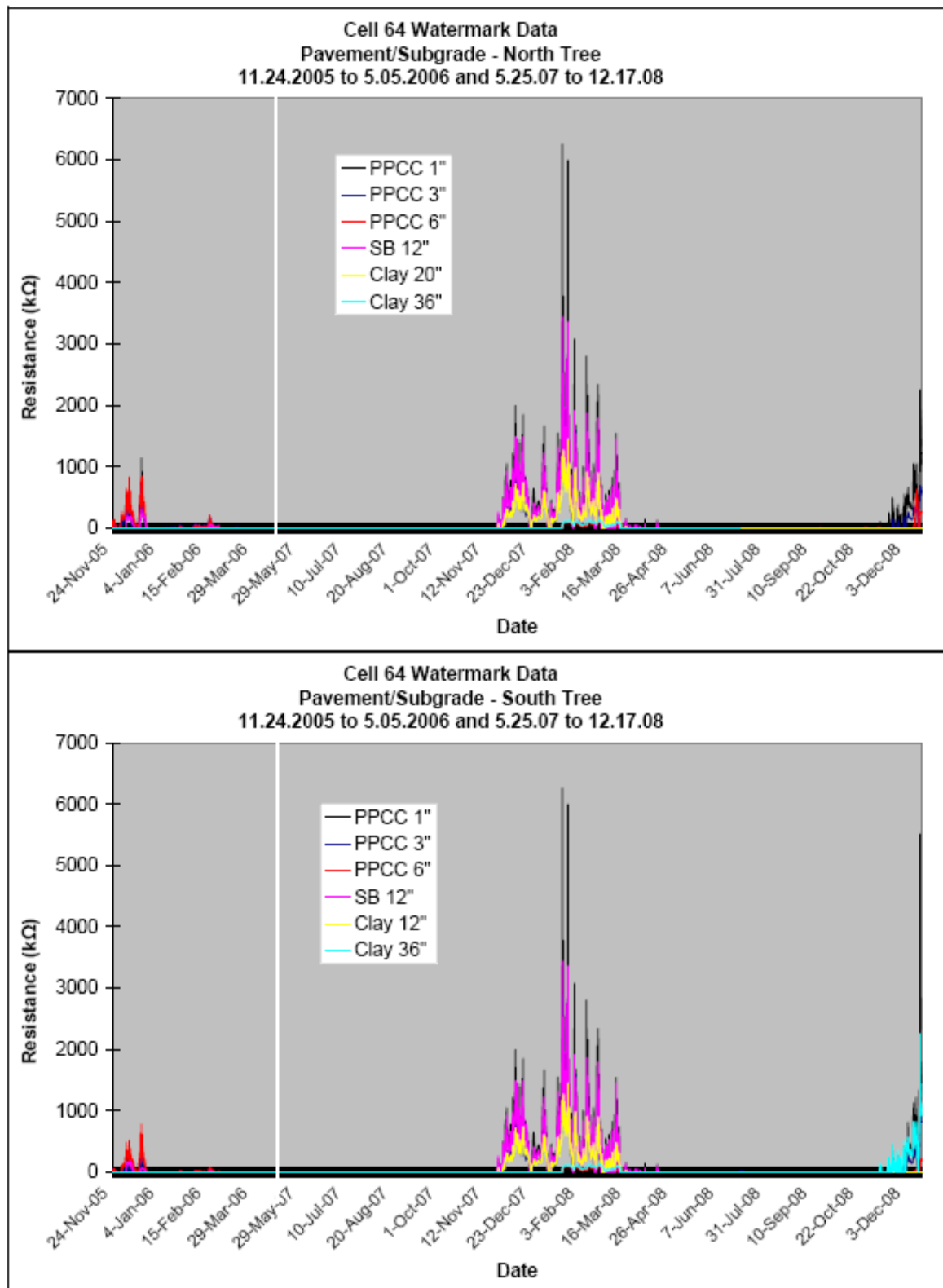


FIGURE 10: Freeze-thaw cycles measured by watermarks in pavement, base, and subgrade.

Watermark sensors have been installed at MnROAD to count freeze-thaw cycles for many years. These sensors are typically used in agricultural applications to measure soil water saturation. They are helpful in measuring freezing in pavements because when the moisture in the soil surrounding the sensors changes state from liquid to solid, the sensor measures a spike in resistance as shown in Figure 10. The difficulty is determining how high the resistance spikes when this phase change occurs. For the purpose of counting freeze-thaw cycles in this report, a resistance spike above $1.5\text{ k}\Omega$ was used to indicate freezing. This value was chosen because it was just slightly higher than the maximum measured resistance during the three summers since Cell 64 was constructed. A comparison between different definitions of freeze-thaw cycles was made in Figure 11 at various depths below the pavement surface in Cell 64. The different definitions were:

- WM – watermark, using a spike in resistance above $1.5\text{ k}\Omega$
- 0° C – counting every fluctuation above/below 0° C as one cycle
- Max/Min – counting every time the daily maximum and minimum temperature fluctuates above and below 0° C as one cycle

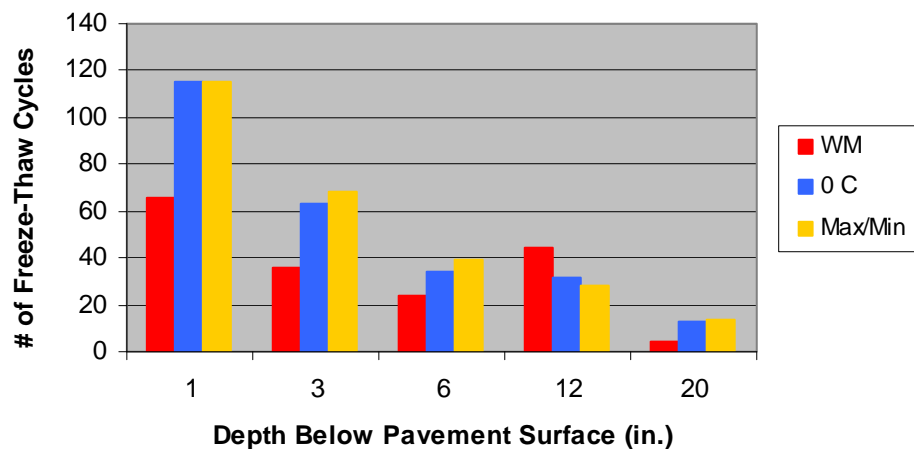


FIGURE 11: Comparison of number of freeze-thaw cycles calculated using different definitions at various depths below Cell 64.

The time period that the freeze-thaw cycles were counted was the winter of 2005/2006, winter of 2007/2008, and 2008 through December 17. No data was available for the winter of 2006/2007. As shown in Figure 10, the 0° C and Max/Min methods using thermocouple sensors gave a similar number of freeze-thaw cycles and the watermark sensors (WM) typically measured fewer cycles. This could indicate that both procedures using thermocouples measure more cycles than are occurring.

The number of freezing cycles measured using thermocouple data is shown in Figure 12 at various vertical depths below the pavement surface for the winters of 2005/06, 2007/08, and 2008/09 through March 1. Temperature data was not collected during the winter of 2006/07. One freezing cycle was defined as a fall and rise above 0 °C. While this is a very simple definition, and may not represent the true number of freeze-thaw cycles, this method can be used as an effective comparison between different pavements.

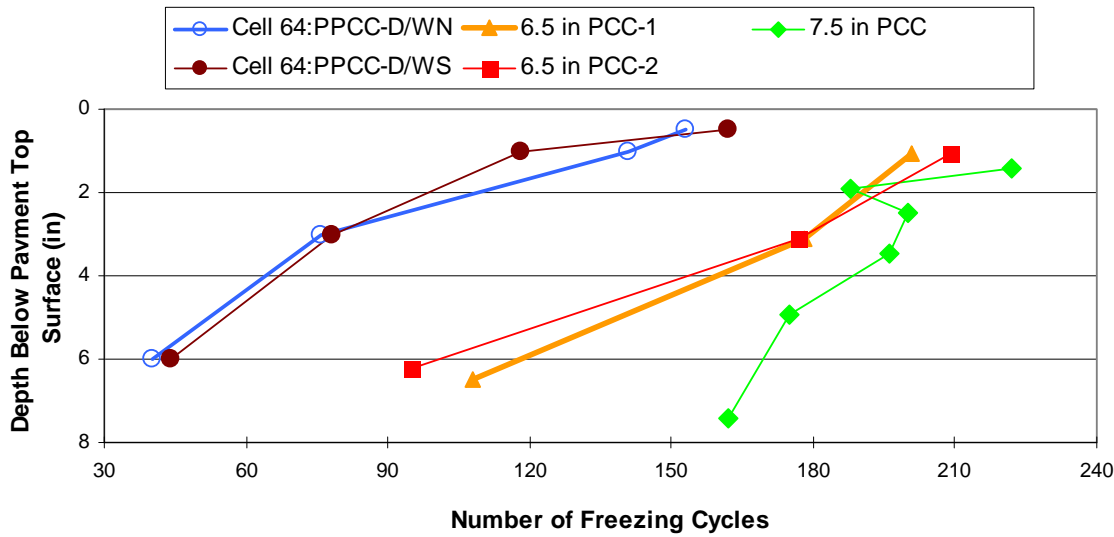


FIGURE 12: Number of freezing cycles at various depths below pervious and impervious PCC pavements of similar thickness.

The data from two different thermocouple trees in the 7 in. thick pervious PCC test Cell 64 is shown in the figure; a north (Cell 64:PPCC-D/WN) and south tree (Cell 64:PPCC-D/WS). Three other impervious PCC pavements of similar thickness are also shown, two 6.5 in. thick and one 7.5 in. thick pavement. Pervious Cell 64 experienced 130 freezing cycles at 1 in. below the top pavement surface. The two 6.5 in. thick pavements experienced 205 (58% increase) and the 7.5 in. thick pavement experienced 222 (72% increase) freezing cycles at 1 and 1.5 in., respectively, below the top pavement surface. At pavement mid depth, the pervious pavement experienced 77 freezing cycles compared to 177 (130% more) in the two 6.5 in. thick and 196 (150% more) in the 7.5 in. thick PCC pavements.

This reduction in freezing cycles experienced by pervious PCC Cell 64 may indicate that even with decreased laboratory-measured freeze-thaw durability of the pavement materials (ASTM C 666), field (actual) freeze-thaw durability of the roadway may be comparable to impervious roadways due to fewer experienced pavement freeze-thaw cycles.

Backstrom [7] attributed an increased temperature in permeable pavements to two causes; increased subgrade temperature due to elevated moisture content and an insulating effect from the air trapped in the permeable pavement. While Cell 64 did not have the required sensors to

accurately monitor subgrade moisture content, Figure 13 shows that the subgrade was warmer during the winter and cooler in the summer in Cell 64 than in Cell 38, a 6.5 in. thick impermeable concrete pavement. Increased subgrade moisture content could explain this phenomenon.

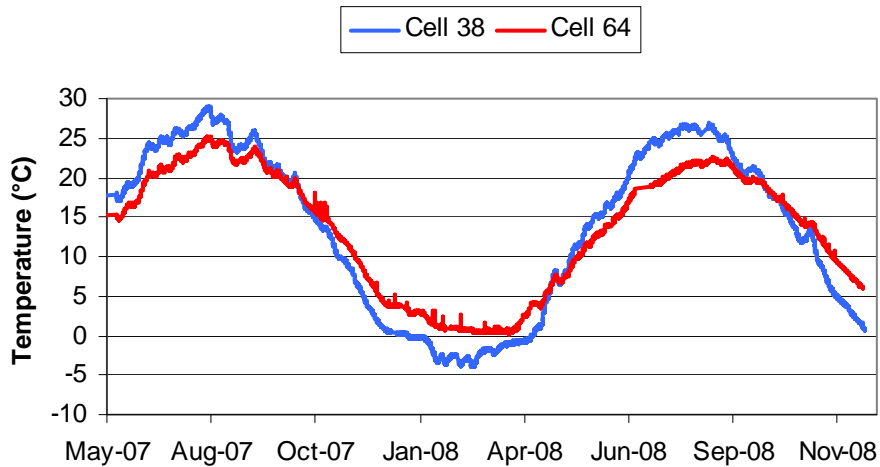


FIGURE 13: Temperature 36 in. below pavement surface.

Figure 14 shows the temperature at mid depth for Cells 64 and 38. The rate of temperature change was much less in Cell 64 than Cell 38. This could be caused from increased insulation due to the air within the pervious concrete. The trapped air keeps the pervious concrete at a more consistent temperature than the impervious Cell 38. The warmer subgrade, which warms from below, and the insulating effect of the trapped air in the pervious concrete both contribute to fewer freeze-thaw cycles in Cell 64 compared to test cells of similar thickness at MnROAD.

Since the primary concern with pervious pavements in Minnesota is freeze-thaw durability, the fact that Cell 64 experienced less freeze-thaw cycles than standard pavements of similar thickness is significant. While the durability of pervious concrete may be low as measured by laboratory test such as ASTM C 666, in the field it may have good durability due to fewer experienced freeze-thaw cycles than impermeable pavements.

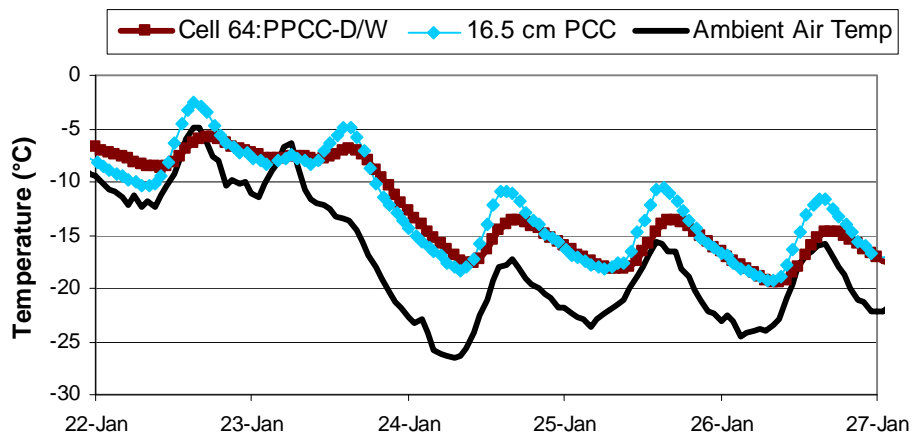


FIGURE 14: Mid-depth temperature in pervious (PPCC) and impervious (PCC) test cells at MnROAD.

CONCLUSION

The main change in surface distress from the first year to the third year of service was the presence of a longitudinal crack that extended the length of Cell 64 and severe raveling in some portions of Mix #2. Initiating at the pole barn at a joint in the concrete curb, the longitudinal crack could have propagated the length of Cell 64 due to FWD, traffic, or thermal loading. Present in the 2006, 2008, and 2009 distress surveys was spalling at tooled joints and surface raveling of Mix #2. The portion of Mix #2 that raveled after the first winter does not seem to be worsening. The highest measured Schmidt hammer values were at the raveled portion of Mix #2. This indicated that Mix #2 did not ravel due to low strength.

The inverted Humboldt H-4245 sand cone works well to measure changes in the hydraulic conductivity. A threshold of 5 min. was used to determine clogging. Measurements made before and after Cell 64 was swept indicate that sweeping decreases hydraulic conductivity and can causes clogging. Further changes in hydraulic conductivity will be monitored seasonally and after significant rainfall or maintenance events.

Freeze-thaw cycles were monitored by analyzing the data from two sensor trees of watermarks and thermocouples within the pavement and subgrade. The number of freeze-thaw cycles at different depths in the pavement was compared between Cell 64 and other concrete and HMA pavements of similar thickness at MnROAD. It was found that the pervious concrete of Cell 64 experience less freeze-thaw cycles than impermeable pavements of similar thickness. The subgrade in Cell 64 also stayed warmer during the winter and cooler in the summer. This could have happened due to higher moisture content in the subgrade than in impermeable pavements. The air trapped between the voids in the pavement also could have helped to insulate the pervious concrete.

Changes in hydraulic conductivity, surface distress, and strength (Schmidt hammer) will continue to be monitored. Knowledge of pervious concrete will greatly be expanded with the testing of Cells 85, PCC pervious on sand, and 89, PCC pervious on clay, on the MnROAD Low Volume Road.

REFERENCES

1. B.I. Izevbekhai, T. Burnham, B. Worel, K. MacDonald, B. Burke, and D.P. Frentress. (2005). *2005 MnROAD – Pervious Concrete Project: Cell-64 Driveway Construction Report*, Minnesota Department of Transportation, St. Paul, MN.
2. A.J. Eller and B.I. Izevbekhai. (2007). *MnROAD Cell 64 Pervious Concrete First Year Performance Report*, Report No. MN/RC-2007-17, Minnesota Department of Transportation, St. Paul, MN.
3. Digid-Schmidt 2000 Model ND/LD Operating Instructions. (2006). *Proceq USA, Inc.*, Aliquippa, PA.
4. V.R. Schaefer, K. Wang, M.T. Suleiman, and J.T. Kevern. (2006). *Mix Design Development for Pervious Concrete in Cold Weather Climates*, Report No. 2006-01. Center for Transportation Research and Education, Iowa State University, Ames, IA.
5. J.D. Luck, S.R. Workman, S.F. Higgins, and M.S. Coyne. (2006). *Hydrologic Properties of Pervious Concrete*, Transactions of the ASABE, Vol. 49, No. 6, pp. 1807-1813.
6. F. Montes and L. Haselbach. (2006). *Measuring Hydraulic Conductivity in Pervious Concrete*, Environmental Engineering Science, Vol. 23, No. 6, pp. 960-969.
7. M. Backstrom. (2000). *Ground Temperature in Porous Pavement During Freezing and Thawing*, Journal of Transportation Engineering, Vol. 126, No. 5, pp. 375-381.

APPENDIX A

MNROAD TEST SECTIONS

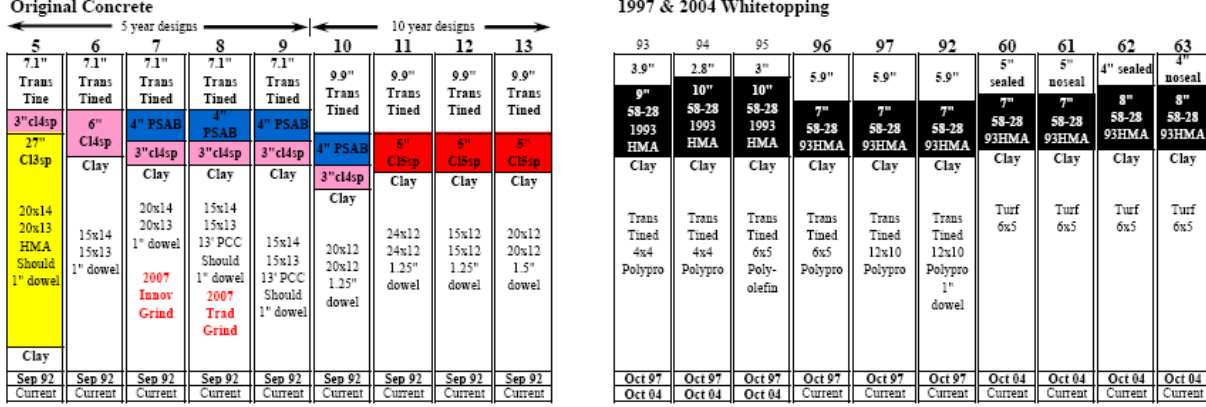
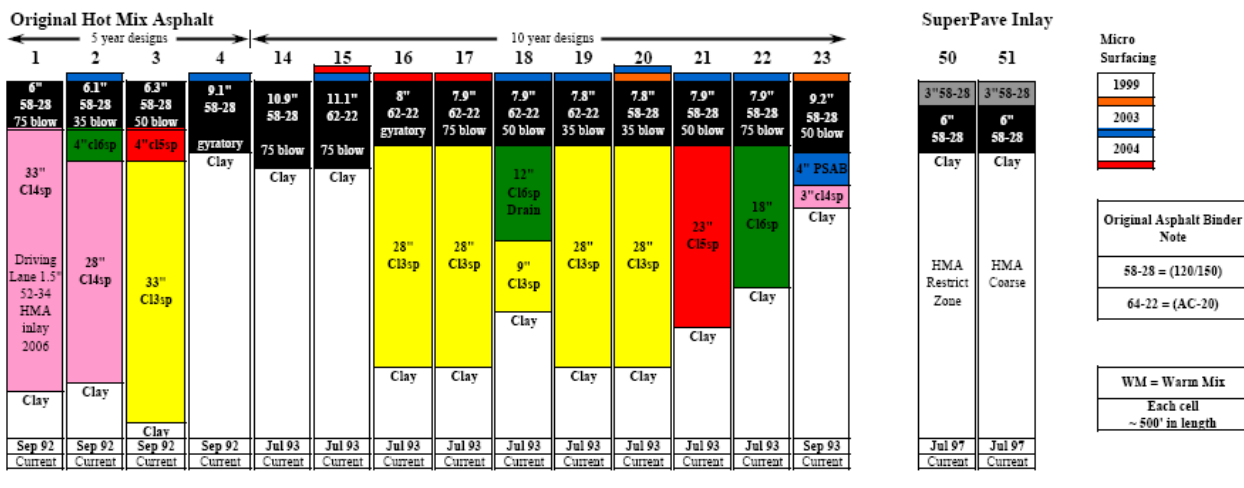
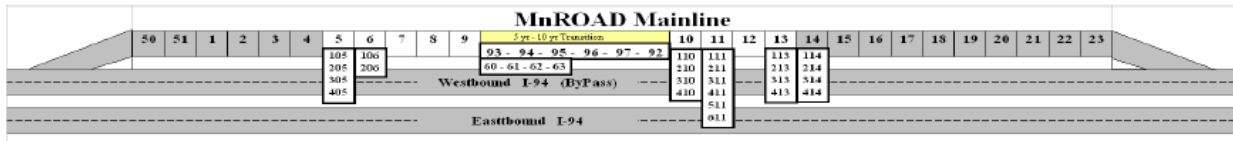


FIGURE A-1: MnROAD Phase I Mainline test sections.

Full Depth Reclamation			LTC	Unbound Overlay Recycled Base			Low Temp Cracking			Mesabi Stone Base	Unbonded PCC Overlay	Composite				
2	3	4	15	16	17	18	19	20	21	22	105	205	305	405	106	206
2"64-34	2"64-34	2"64-34	3" WM	5" WM	5" WM	5" WM	5" WM	5" WM	5" WM	5" WM	4"	4"	5"	5"	2"64-34	2"64-34
6" FDR treated	6" FDR treated	8" FDR treated	58-34	58-34	58-34	58-34	58-34	58-28	58-28	58-34	7.1"	7.1"	7.1"	7.1"	6"	6"
6" FDR	6" FDR	9" FDR + Fly Ash	11.1" 64-22 1993 HMA	12" 100% recycle PCC	12" 50% RePCC 50% Class 5	12" 100% RAP	12" Cl-5	12" Cl-5	12" Cl-5	12" Mesabi Ballast	cracked '93 PCC	cracked '93 PCC	'93 PCC	'93 PCC	Cl-5	Cl-5
26" Cl4sp	33" Cl3sp		Clay	12" Cl3sp	12" Cl3sp	12" Cl3sp	12" Cl3sp	12" Cl3sp	12" Cl3sp	12" Cl3sp	27" Cl3sp	27" Cl3sp	27" Cl3sp	27" Cl3sp	6" Clay Borrow	6" Clay Borrow
Clay			58-34 Surface Binder	7" Select Gran	7" Select Gran	7" Select Gran	7" Select Gran	7" Select Gran	7" Select Gran	7" Select Gran	Orig 20x14	Orig 20x14	Orig 20x14	Orig 20x14	Mesabi 4.75 SuperP	Mesabi 4.75 SuperP
			Clay	Clay	Clay	Clay	Clay	Clay	Clay	Clay	20x13 HMA Should 1" dowel	15'x12' 1" dowel	15'x12' no dowels			
2008	2008	2008		2008	2008	2008	2008	2008	2008	2008	2008	2008	2008	2008	2008	2008

Trapezoidal Concrete Design				Subgrade Drag Tie Bar Design				Thin Concrete				2008 Whitetopping					
110	210	310	410	111	211	311	411	511	611	113	213	313	413	114	214	314	414
10	10	10	10	11	11	11	11	11	11	13	13	13	13	14	14	14	14
6"-8" drive pass	6"-8" drive pass	6" CI-8	6" CI-8	7" CI-8	7" CI-8	7" long broom	7" long broom	7" long broom	7" long broom	5"	5.5"	6"	6.5"	6" light turf	6" light turf	6" light turf	6" light turf
0" CI-8	0" CI-8	6" CI-8	6" CI-8	6" CI-8	6" CI-8	6" CI-8	6" CI-8	6" CI-8	6" CI-8	5" CI-5	5" CI-5	5" CI-5	5" CI-5	5" 58-28 93 HMA	6" 58-28 93 HMA	7" 58-28 93 HMA	8" 58-28 93 HMA
Clay	Clay	Clay	Clay	Clay	Clay	Clay	Clay	Clay	Clay	Clay	Clay	Clay	Clay	Clay	Clay	Clay	Clay
heavy burlap	heavy burlap	heavy burlap	heavy burlap	15'x12' 1" dowel 3#5 tie	heavy turf	heavy turf	heavy turf	heavy turf	6"x6' 1" dowels driving								
15'x12' 1" dowel 3#5 tie	15'x12' 1" dowel 3#5 tie	15'x12' 1" dowel 3#5 tie	15'x12' 1" dowel 3#5 tie	10' PCC should 1" dowel 3#13 ties	15'x12' 1" dowel 5#19 ties	no dowels passing	no dowels passing	no dowels passing	no dowels passing								
2008 or 2009	2008 or 2009	2008 or 2009	2008 or 2009	2008 or 2009	2008 or 2009	2008 or 2009	2008 or 2009	2008 or 2009	2008 or 2009	2008	2008	2008	2008	2008	2008	2008	2008

FIGURE A-2: MnROAD Phase II Mainline test sections.

MnROAD Low Volume Road

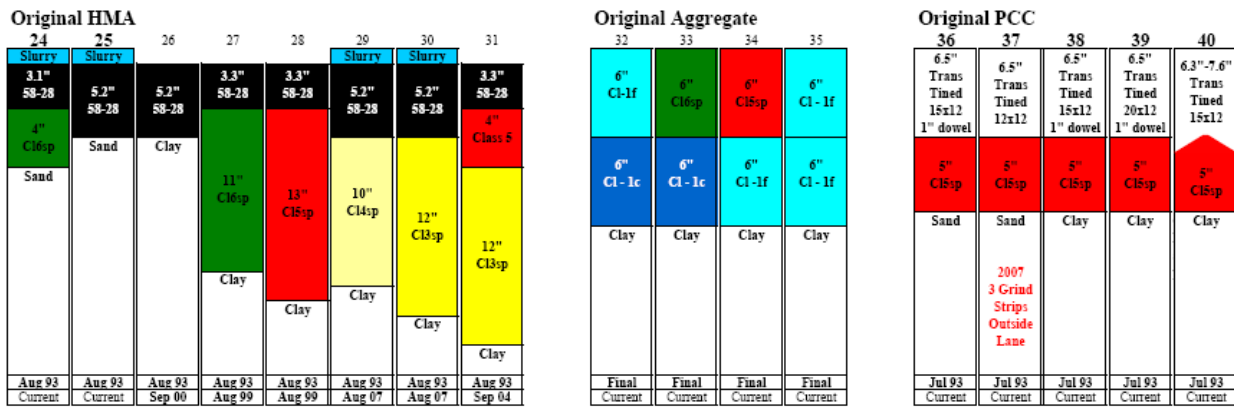
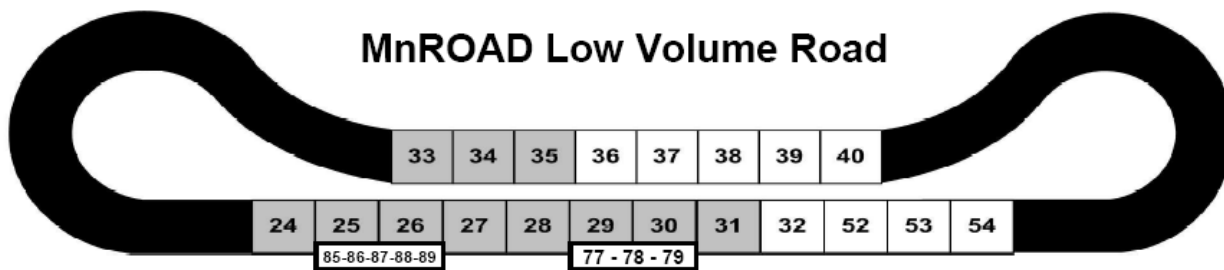


FIGURE A-3: MnROAD Phase I Low Volume Road (LVR) test sections.

HMA Constructed					PCC Constructed					60-Year PCC					Mesabi Hard Rock			60" Culverts		Geocomposite Barrier Drain		
2.5 Oil Gravel	26	26	27	27	2.5 Oil Gravel	2.5 Oil Gravel	2.5 Oil Gravel	2.5 Oil Gravel	2.5 Oil Gravel	5"	Astro Turf	7.5"	Astro Turf	7.5"	12"	4"	7.5"	60"	4"	27	28	
8" FDR		4" 58-28	2X Chip		14" Large Stone	14" Large Stone	14" Large Stone		14" Large Stone	5"	Turf 10x12	Var Dowels	Turf 15x13/14	Turf 15x13/14	Stamped 15x12	64-34	Astro Turf	Culverts	58-28	52-34	52-34	
Clay			Clay		Clay	Clay	Clay		Clay	6"	CI-1f	6.5" 20x12	5" CI4sp	5" CI4sp	1.5" SS dowels	CI4sp	15x12'	60" Plastic PCC Steel Culverts	58-34	58-34	58-34	
Sep 00	May 04	Aug 99	Sep 00	Aug 99	Sep 00	Aug 06	Aug 06		Aug 06	32	39	4" Perv Overlay	7.5" Astro Turf	7.5" Astro Turf	12" PCC Should	4" Cl-5	7.5" Astro Turf	Hard Rock	4"	4"	4"	
May 04	Current	Current	Sep 00	Aug 06	Aug 06	Jun 00	Jun 00		Jun 00	39	52	6.5" 20x12	5" CI4sp	5" CI4sp	1.5" SS dowels	12" CI6sp	15x12'	60" Plastic PCC Steel Culverts	58-34	52-34	52-34	
						Jun 00	2008		Jun 00	53	53	1" dowel	Clay	Clay	Clay	36" SG	12" CI6sp	Hard Rock	4"	4"	4"	
						Current			Jun 00	31	54	PCC Should	Clay	Clay	Clay	Clay	Clay	60" Plastic PCC Steel Culverts	58-34	52-34	52-34	
						Current			Jun 00	31	54	Clav	Clav	Clav	Clav	Clay	Clay	Clay	Clay	Clay	Clay	
						2008			2008			Sep 04	Oct 04	Oct 04	Oct 04	Oct 04	Oct 04	Oct 04	Oct 04	Aug 06	Aug 06	Aug 06
						Current			Current			Current	Current	Current	Current	Current	Current	Current	Current	Current	Current	Current

Pervious Full Depth				Fly Ash Stabilization				1999 SuperPave				Acid Modified				Implements of Husbandry			
Park Lot	Sidewalk	85	86	87	88	89	77	78	79	33	34	35	33	34	35	83	84		
64	74	25	25	25	26	26	4" Perv PCC	5" Perv HMA	4" Control	4" 58-34	4" 58-34	4" 58-34	4" 58-34	4" 58-34	4" 58-34	4" 58-34	5.5" 58-34		
7"	Perv PCC	6"	Washed Stone	7"	Perv HMA	7"	Perv PCC	14" CA-15	15" CA-15	14" CA-15	14" CA-15	12" CA-15	8" FDR	8" CI6sp	8" FDR Fly Ash	12" CI6sp	12" CI6sp	9" CI-5	
12" CA-15	Type V Geo-Textile	12" CA-15	14" CA-15	15" CA-15	14" CA-15	12" CA-15	Clay	Type V Geo-Textile	Clay	Clay	Clay	12" CI6sp	12" CI6sp	Clay					
Type V Geo-Textile	Clay	Type V Geo-Textile	Type V Geo-Textile	Type V Geo-Textile	Type V Geo-Textile	Type V Geo-Textile	Sand	Sand	Clay	Sand	Clay	Clay	Clay	Clay	Clay	Clay	Clay	Clay	
Clay		2008	2008	2008	2008	2008	2008	Oct 07	Oct 07	Sep 07	Jul 99	Jul 99	Jul 99	Sep 07	Sep 07	Sep 07	Oct 07	Oct 07	
		Current	Current	Current	Current	Current	Current	Current	Current	Jul 07	Jul 07	Jul 07	Jul 07	Jul 07	Jul 07	Jul 07	Current	Current	

FIGURE A-4: MnROAD Phase II Low Volume Road (LVR) test sections.

APPENDIX B

MN/DOT PETROGRAPHIC ANALYSIS REPORT



Minnesota Department of Transportation

MEMO

Office of Materials
Mailstop 645
1400 Gervais Avenue
Maplewood, MN 55109

DATE: April 13, 2006

TO: Bernard Izevbekhai
Concrete Research Engineer

FROM: Nancy Whiting, MSCE
Geologist/Concrete Researcher

PHONE: 651-779-5603

SUBJECT: Petrographic analysis of pervious concrete test pads at MnRoad

Background

Cell-64 "Pole Barn Pervious Concrete Driveway" was placed in September 2005. Just prior to placing the driveway two test pads of pervious concrete were place adjacent to the driveway. The intention of the test pads was to place similar mixes and practice placement techniques. As with the driveway, the test pads were exposed to environmental stresses such as wetting/drying and freeze/ thaw cycles throughout the fall and winter.

Four cores were taken from the pervious concrete test pads in early spring, two from each of test pad adjacent to the pervious concrete driveway (see figure 1). These four cores, identified as 6406CC001, 002, 003 and 004 were submitted for petrographic analyses and will hence be referred to as cores 1, 2, 3 and 4 respectively. Concern was expressed as to the air void content (porosity), mix design, durability and possible segregation of the mixes.

Additional cores were taken from cell-64, the pervious concrete driveway, and Cemstone performed a petrographic analysis of these cores. Kevin MacDonald presented some of these results at the Minnesota Concrete Council's annual meeting, on March 16, 2006. It appears that the pervious concrete placed in the driveway differed from that placed in the test pads on some key characteristics. For example, the air void system and paste content differed. Therefore, the following analyses represents the test pads only and not the concrete in cell-64, pervious concrete driveway.

Megascopic Examination

Core 1 was taken from the same test pad and less than 2 ft from core 2. Megascopically they appeared very similar, therefore only one core, core 2 was chosen to examine microscopically to represent the mix that was poured in this test pad. Cores 3 and 4 were taken from the other test pad, appeared difference from cores 1 and 2, but similar to each other. Core 3 was chosen to represent the mix poured for that test pad.

Photos and the megascopic observations for cores 2 and 3 are detailed in the attached appendix. In summary, each test pad represents a distinctly different mix. The coarse aggregate (CA) in cores 1 and 2 was a $\frac{1}{2}$ " minus rounded gravel, and in cores 3 and 4 was a $\frac{3}{8}$ "minus angular quarried carbonate coarse aggregate. Both mixes were matrix supported with very little to no evidence of point-to point contact of the coarse aggregates. There was slightly more paste surrounding the $\frac{3}{8}$ "minus quarried carbonate CA in cores 3 and 4, then surrounding the $\frac{1}{2}$ " minus gravel CA in cores 1 and 2.

Both mixes contained sand, showed no segregation in the aggregate size and quantity with depth but some segregation in both size and quantity of the air voids. There were obviously fewer voids near the surface of the concrete in cores 3 and 4 while the decrease of voids near the surface in cores 1 and 2 were only slightly noticeable.

To more precisely quantify the air void system and other mix design parameters, slabs were cut and polished from cores 2 and 3 to represent concrete near the surface, at mid-depth and near the bottom of the test pad (as shown in figure 2). ASTM C457 Linear Traverse was performed on each slab. Table 1 summarizes the results.

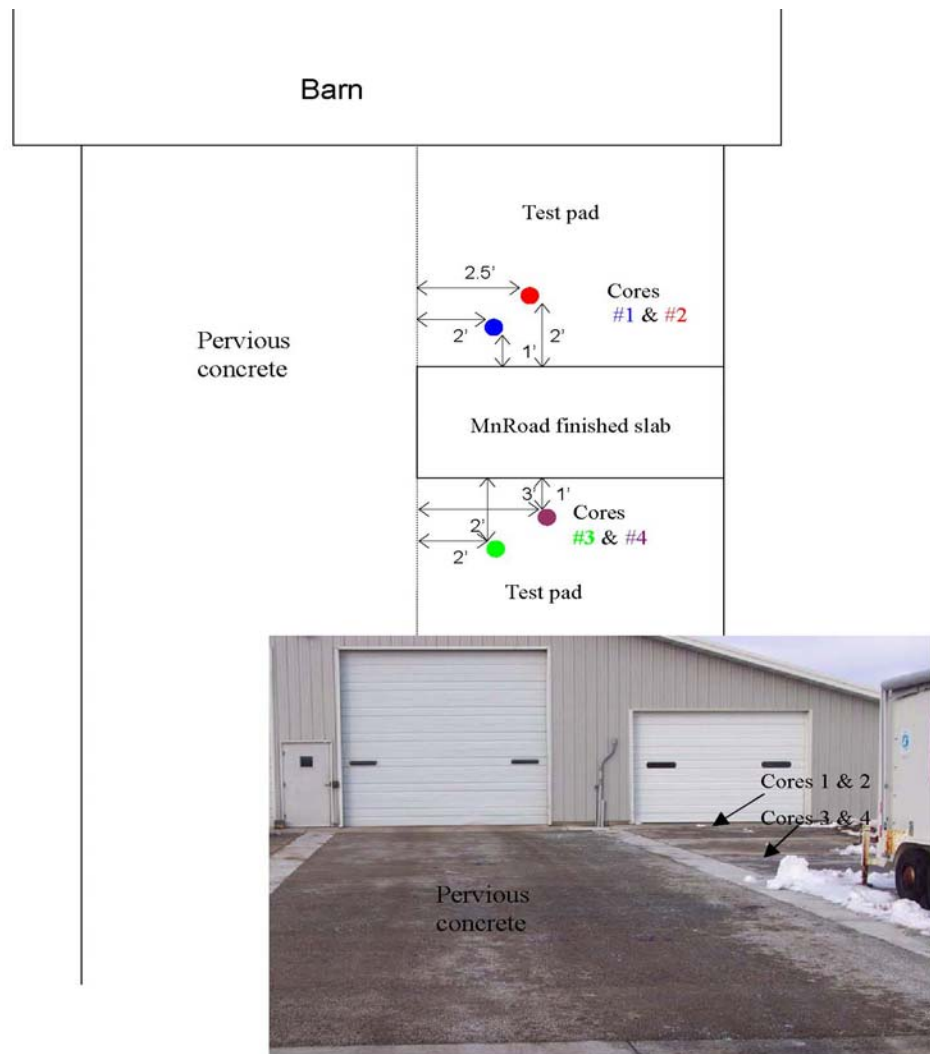


FIGURE B-1: Schematic and photo showing the layout of the pervious concrete at MnRoad. Cell-64 Pervious Concrete Driveway is in foreground, test pads are to the far right (schematic is not to scale).

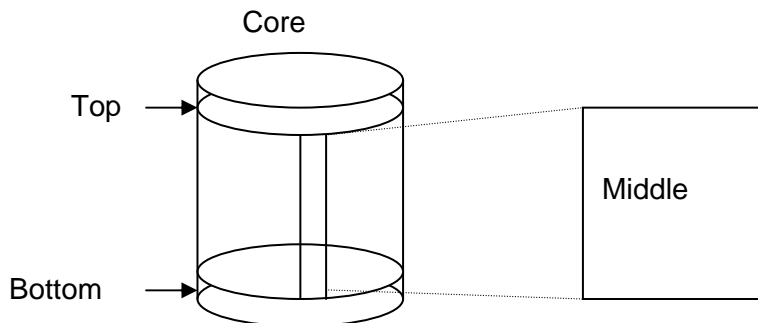


FIGURE B-2: Illustration of how cores are sectioned for microscopic evaluation.

TABLE B-1: Air Void System Analysis Results per ASTM C457 Linear Traverse

	Core #2 (CA = 1/2" rd gravel)				Core #3 (CA = quarry carbonate)			
	Top 1"	Middle 3.5"	Bottom 1"	Design	Top 1"	Middle 3.5"	Bottom 1"	Design
% Total Air	8.3	11.7	11.8	33 (20.2**)	4.9	17.5	22.4	33 (26.7**)
% Paste	23.9	24.8	22.9		30.8	27.7	24.8	
%Agg	67.8	63.5	65.3		64.3	54.9	52.8	
Paste:Void ratio	2.9	2.1	1.9		6.2	1.6	1.1	
%Entrained	0.5	0.2	0.8		1.1	0.8	0.6	
Spacing factor (in)	0.017	0.029	0.016	< 0.008*	0.013	0.015	0.014	< 0.008*
Specific Surface (in ² /in ³)	166	73	123	≥ 600*	396	109	79	≥ 600*

*PCA recommendation for F/T resistance OPC concrete in severe climates

** Plastic air content in lab specimens

Microscopic Observations

Both mixes contained sand, although the quantity of sand was less than a conventional PC concrete contains. Also, there were fewer entrained air voids than a well air-entrained conventional PC concrete needs for freeze/thaw resistance in MN.

Air void system

As shown in Table 1 the linear traverse analyses supports and quantifies the general observations of the air void system. Only small percentage of the air was entrained air at $\leq 1\%$, and the spacing factor was much lower than recommended for freeze/thaw resistance for conventional PC concrete in both cores. In calculating the specific surface, it is assumed that the air voids are spherical; therefore, comparing these values in pervious concrete to accepted standards is not accurate or valid.

As seen megascopically the air void distribution shows some slight segregation in core 2, having slightly less air in the top inch (8.3%) then in the middle (11.7%) and bottom of the core (11.8%). The air voids are much more segregated in Core 3, having much less air in the top (4.9%) and clearly more air with depth, increasing to 17.5% in the middle and 22.4% at the bottom.

Cracks

Polished slabs were examined under the stereomicroscope. Fine tight cracks were apparent under low magnification in both cores at all depths. In core 2 the cracks were predominantly through the paste running from air void-to-air void, air void-to-aggregate and/or aggregate-to-aggregate (as shown in figure 3). Occasionally the cracks would follow the aggregate-paste interface. Only rarely were cracks through aggregate particles. There was no visible difference in the abundance of cracks with depth.

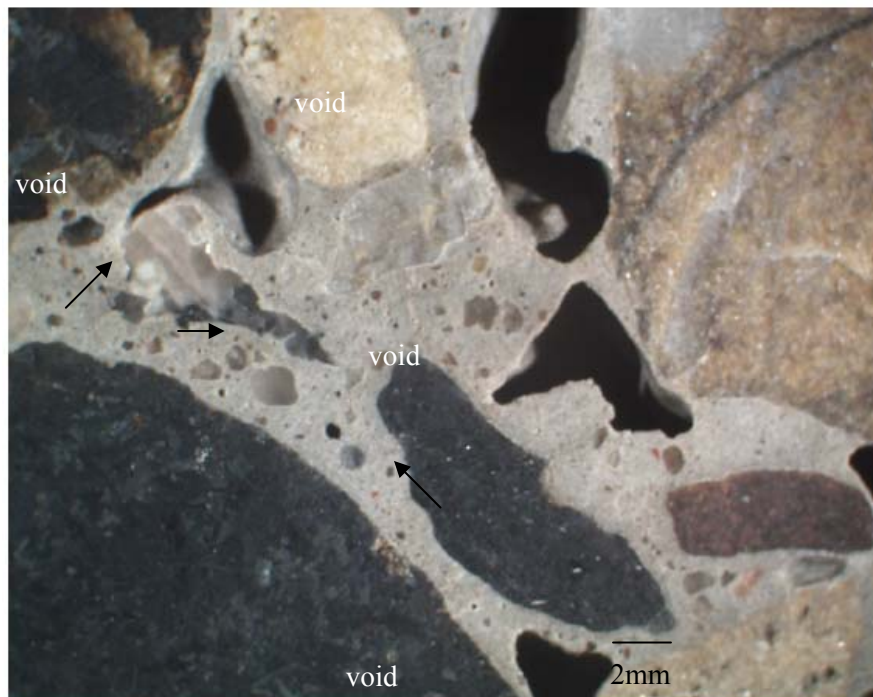


FIGURE B-3: Arrows point to fine cracks in paste in core 2.

In core 3 the cracks commonly ran through the aggregates as well as through the paste, as seen in Figure E4, more abundant near the top then near the bottom of the core. Cracks were more apparent near the top of core 3 than in core 2.

It is difficult to determine precisely what has caused these cracks, but some possibilities to consider include: 1) environmentally induced from exposure to repeated freeze/thaw cycles, 2) possibly shrinkage from the low w/cm ratio contributed to some cracking, or 3) lower strengths resulted in some mechanical failure from heavy loads.

The fact that there are more cracks in the top portion of core 3 which had a much higher paste:void ratio and much lower air content than any other concrete suggests that freeze/thaw may have contributed. If strength was an issue then the portion of the mix with higher air, such as the bottom of core 3, would have been weaker and shown more distress/cracks. The higher

paste content at the top of core 3 may have led to higher internal stresses caused by drying and shrinkage, but this would not explain cracks that run through the aggregate too.

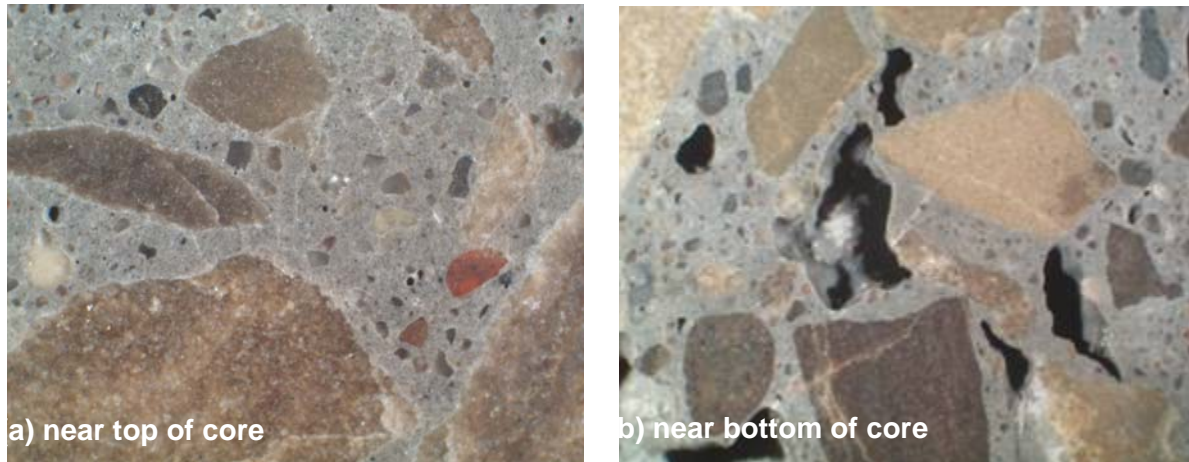


FIGURE B-4: Microscopic view of polished slabs from core 3 showing several fine tight cracks. Note the lack of air voids and numerous cracks at the top (a) compared to the more abundant air and fewer cracks through paste in the bottom (b) of the slab.

Summary

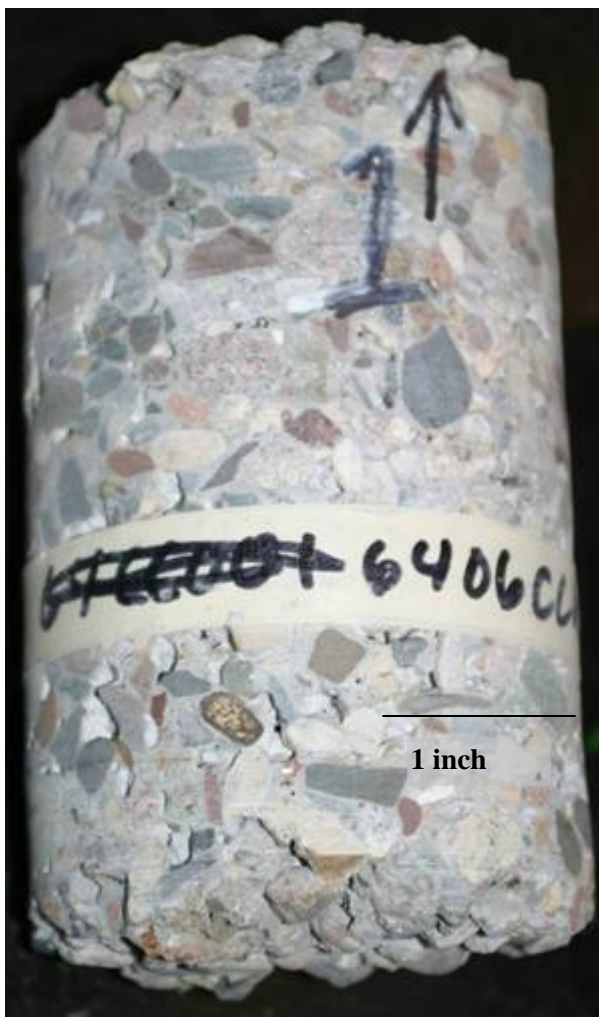
The pervious concrete in each test pad have different characteristics most noticeably different air-void systems. One test pad, as represented by cores 1 and 2 had fairly uniform amounts of air with depth, but total air was much lower than anticipated or designed. The other test pad had a higher total air content, but the amount of air was not well distributed with depth, with the air in the top of the slab greatly reduced. These differences may be the results of using different aggregate size, shape and/or types; different mix designs; any differences in placement techniques; and/or how the different mixes responded to placement techniques.

Internal cracks are a problem. The total air was lower than anticipated and the amount of paste surrounding aggregate particles is higher than ideal for pervious concrete. This, along with a very low amount of entrained air in the paste may have reduced the concrete's resistance to freeze/thaw stresses. The portion of the one slab that had the highest amount of paste, and highest paste:void ratio had the most cracks. The presence of cracks reduces the strength of the concrete and increases its susceptibility to environmentally induced distress.

Future Work

Cores 1 and 4 have been set aside and the Foundations Unit will attempt to retrofit their equipment to run permeability tests on these samples.

Appendix



CORES # 1 AND # 2 MEGASCOPIC OBSERVATIONS

3.6" Diameter
5.5" Length (#1)
5.75" Length (#2)

Coarse Aggregate: $\frac{1}{2}$ " top size; primarily rounded gravel, some with crushed faces, mostly fine-grained mafics (igneous and metamorphic), a few coarse-grained igneous and metamorphics, approximately $\leq 20\%$ carbonates (rounded). Not a lot of paste surrounding the aggregates but still matrix supported, very little point-to-point contact of aggregates. No obvious segregation in aggregate content or size. Core #2 is very similar in appearance.

Air void system: Fairly well distributed air void system, with only a slight decrease in size and frequency of voids in top inch.

BASE: NO BASE MATERIAL ATTACHED TO BOTTOM OF CORE #1 BUT SOME SMALL GRAVEL AND SAND ATTACHED TO BOTTOM OF CORE #2.

GENERAL MICROSCOPIC OBSERVATIONS (CORE #2): VERY FEW ENTRAINED AIR Voids OBSERVED. SAND IS PRESENT BUT IN SMALLER

QUANTITIES THAN IN A NORMAL PCC MIX. PASTE IS PRIMARILY A LIGHT-GREY COLOR WITH OCCASIONAL SMALL ZONES OR PATCHES OF A LIGHTER TAN-COLORED PASTE WITH A SLIGHTLY DIFFERENT TEXTURE INDICATING SOME KIND OF SEGREGATION IN THE PASTE (POSSIBLY ZONES OF HIGHER W/CM?). THERE IS EVIDENCE OF FLY ASH IN THE MIX.

Cracks were observed. In the mid-section of the core there were only a few cracks primarily in the paste and at the paste-aggregate interface. Within the top and bottom 1-inch cracks were more pervasive, seen randomly through the paste, from void to void, along the paste aggregate interface and radiating out from voids.



CORES # 3 AND # 4 MEGASCOPIC OBSERVATIONS

3.6" Diameter
6.5" Length

Coarse Aggregate: 3/8-inch top size; primarily carbonates, crushed, angular to subrounded, some sandy and/or silty. Matrix supported - paste surrounding all aggregates, slightly more paste then in cores 1 and 2, and core 3 has slightly more paste then core 4. No apparent segregate in aggregate size or content.

Air void system: Distinct segregation of air voids. The top 2-inches visibly contains fewer and smaller voids then the remaining depth of concrete.

Base: No base material attached to core #4, but core #3 has gravel attached to bottom of core.

GENERAL MICROSCOPIC OBSERVATIONS (CORE #3): THERE

ARE FEW ENTRAINED AIR Voids. SAND IS PRESENT. THERE IS EVIDENCE OF FLY ASH IN THE MIX.

Cracks were observed, especially in the top inch and some in the mid-section, primarily in the paste and through the carbonate aggregate. (as seen in figure)

APPENDIX C

CEMSTONE PETROGRAPHIC ANALYSIS REPORT



To: Dr. Kevin MacDonald

From: Mark Lukkarila

Date: August 9, 2006

Re: Petrographic Analysis, Mn/DOT Cell 64 Pervious Pavement

I am pleased to present the findings of our petrographic analysis performed on four hardened concrete core samples that were obtained and submitted by a representative of the Minnesota Department of Transportation. As received the cores were labeled #1, through #4. It is understood that cores #1 through #3 represent pervious pavement that has deteriorated due to the physical action freezing and thawing while saturated. Core #4 was reported to represent pervious pavement that has not deteriorated to the extent the other areas represented by Sample #1 through #3.. Each sample was examined petrographically in accordance with ASTM C 856.

Sample #	Description
1	Approximately 9.5 cm diameter by 18 cm long concrete core
2	Approximately 9.5 cm diameter by 18 cm long concrete core
3	Approximately 9.5 cm diameter by 17.5 cm long concrete core
4	Approximately 9.5 cm diameter by 16.5 cm long concrete core

Thin section analyses of Samples #1 through #4 revealed a paste composed primarily of residual portland cement and residual fly ash particles along with corresponding hydration products. The water-to-cementitious ratios were interpreted to be low to moderately low (i.e. 0.30 to 0.40) based on the optical and physical properties of the cementitious paste (Photos #1 through #4).

Thin section analyses revealed inhomogeneities within the paste fraction of all of the submitted samples. The inhomogeneities consisted of lower water-to-cementitious ratio paste within pockets of higher water-to-cementitious ratio paste, especially within recesses of the coarse aggregate particles (Photos #5 through #8). These characteristics would be consistent with retempering.

Cracking and microcracking was observed both parallel to, and normal to the top surface. Microcracking oriented parallel to the top surface was observed to depths of approximately 5 cm, 3.5 cm, 7 cm, and 1 cm in Sample #1, #2, #3, and #4, respectively. All samples exhibited extensive microcracking within the top 1 cm, some of which were consistent with severe shrinkage (Photo #9). Carbonation of paste directly adjacent to the microcracks was common. A majority of the microcracks exhibited autogenous healing (Photo #10).

The air void systems in the submitted samples were comprised essentially of compaction voids, which would be consistent with pervious pavement (Photos #11 through #14). The paste fraction was essentially non-air entrained based on the lack of small spherical voids that were less than 1 mm in diameter. Based on abbreviated traverses, the hardened air contents were estimated as follows:

Sample	% Air
#1	21 to 23
#2	28 to 30
#3	24 to 26
#4	29 to 31

The coarse aggregate in Samples #1 and #2 was a glacial gravel combined with crushed dolomite graded up to a ½" size. The coarse aggregate in Sample #3 was a ½" nominal size glacial gravel. The coarse aggregate in Sample #4 was a 3/8" crushed dolomite. The glacial gravel was diverse in lithology with rock types including, but not limited to, carbonate, greywacke, greenstone, siltstone, rhyolite, granite, and sandstone, with some chert and iron oxides. The crushed dolomite was comprised primarily of sparry dolomite with some sandy dolomite. The glacial gravel was mostly subrounded to rounded. As a consequence of quarrying the dolomite was angular.

The fine aggregate was a natural siliceous sand. Whole grains of quartz and feldspar made up a majority of the particles. Lithic rock fragments identified included, but were not limited to, granite, gneiss, schist, greenstone, carbonate, rhyolite, greywacke, basalt, and amphibolite with some chert, iron formation, and opaline shale. The sand was mostly subrounded to subangular.

Methodology

Petrographic examinations, which included examination of polished hand specimens, as well as, thin section analyses, were performed in accordance with ASTM C 856, "Standard Practice for Petrographic Examination of Hardened Concrete." The polished hand specimens are illuminated and examined under a stereoscopic microscope with up to 80X magnification capability. The thin sections are examined using a polarized-light microscope with 500X magnification capability.

The hardened air contents were estimated in accordance with ASTM C 457, "Standard Test Method for Microscopical Determination of Parameters of the Air-Void System in Hardened Concrete", Modified Point Count Method, except abbreviated traverses were performed.

If you should have any questions, or if I may be of further assistance, please contact me at (651) 286-1286.

Sincerely,



Mark R. Lukkarila
Petrographer/Geologist

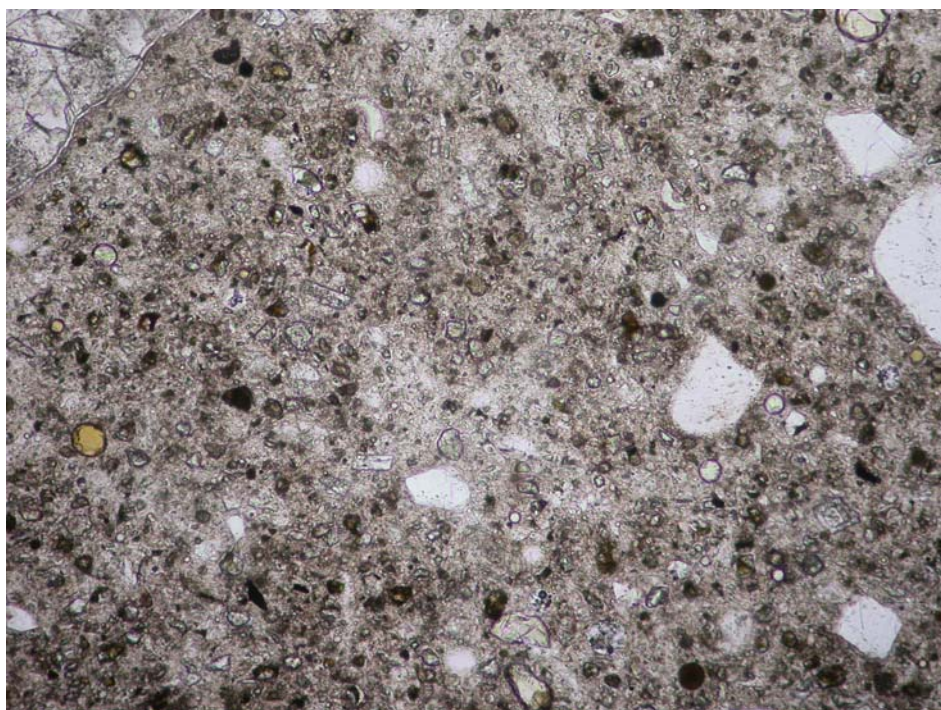


Photo #1: Thin section photomicrograph of the paste in Sample #1. Plane-polarized light;
Field Length = 1.4 mm

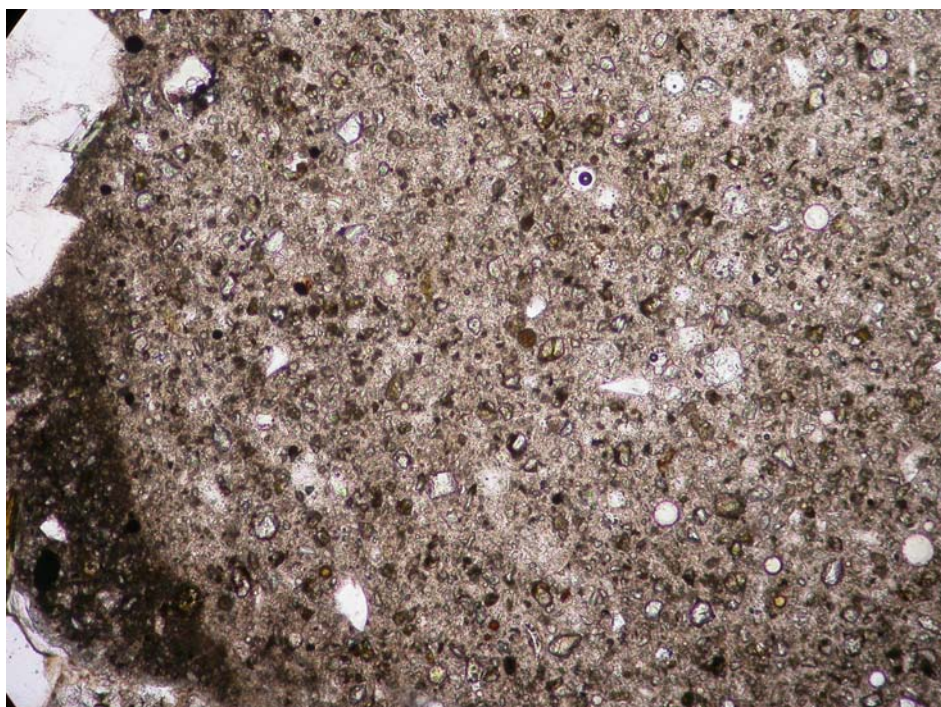


Photo #2: Thin section photomicrograph of the paste in Sample #2. Plane-polarized light;
Field Length = 1.4 mm

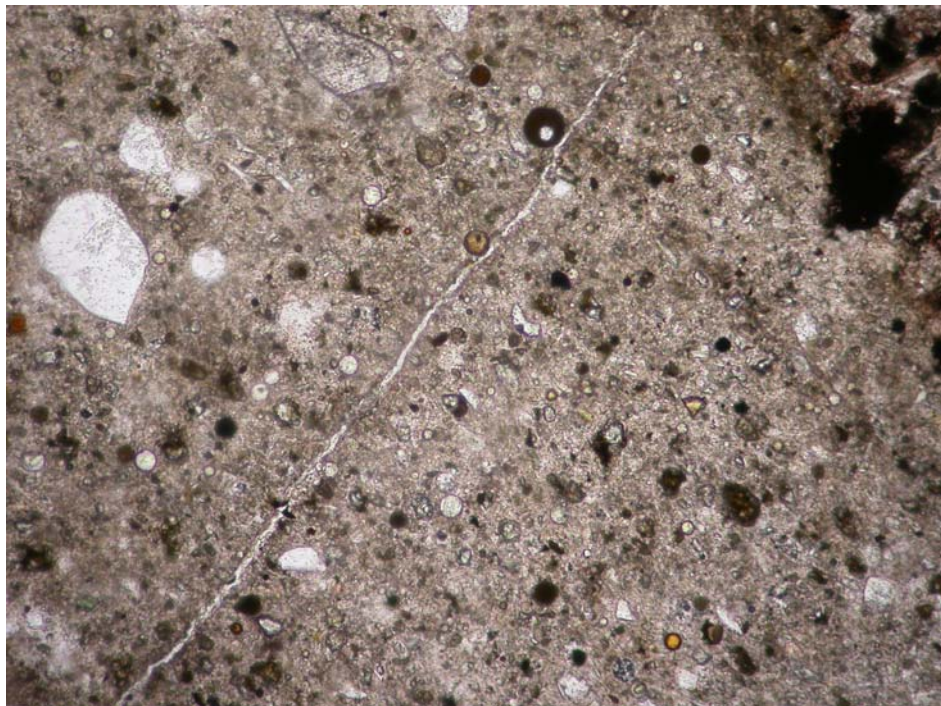


Photo #3: Thin section photomicrograph of the paste in Sample #3. Plane-polarized light;
Field Length = 1.4 mm

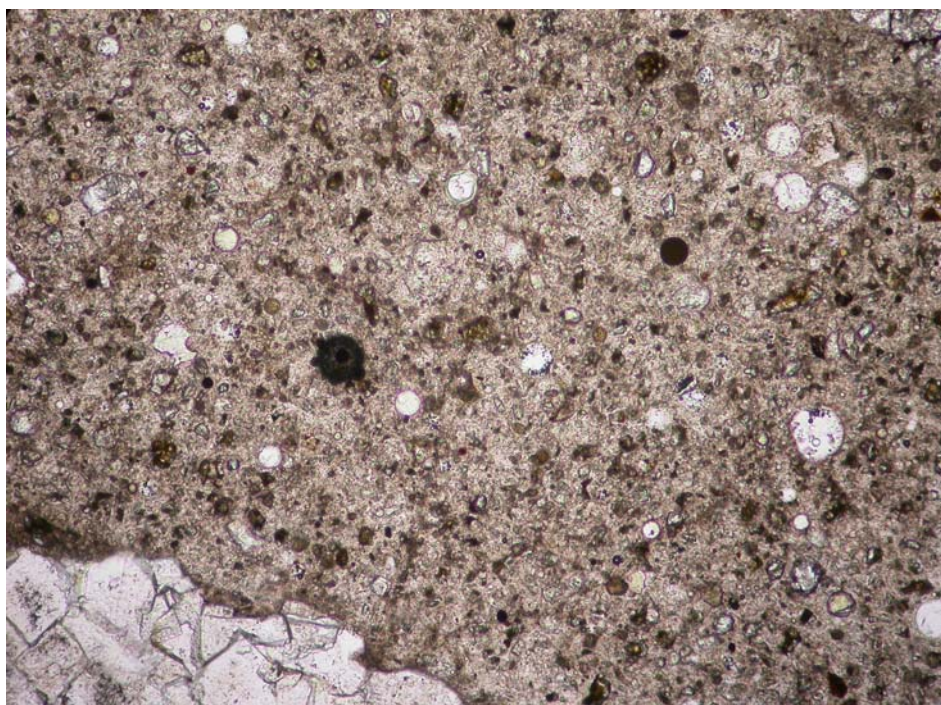


Photo #4: Thin section photomicrograph of the paste in Sample #4. Plane-polarized light;
Field Length = 1.4 mm

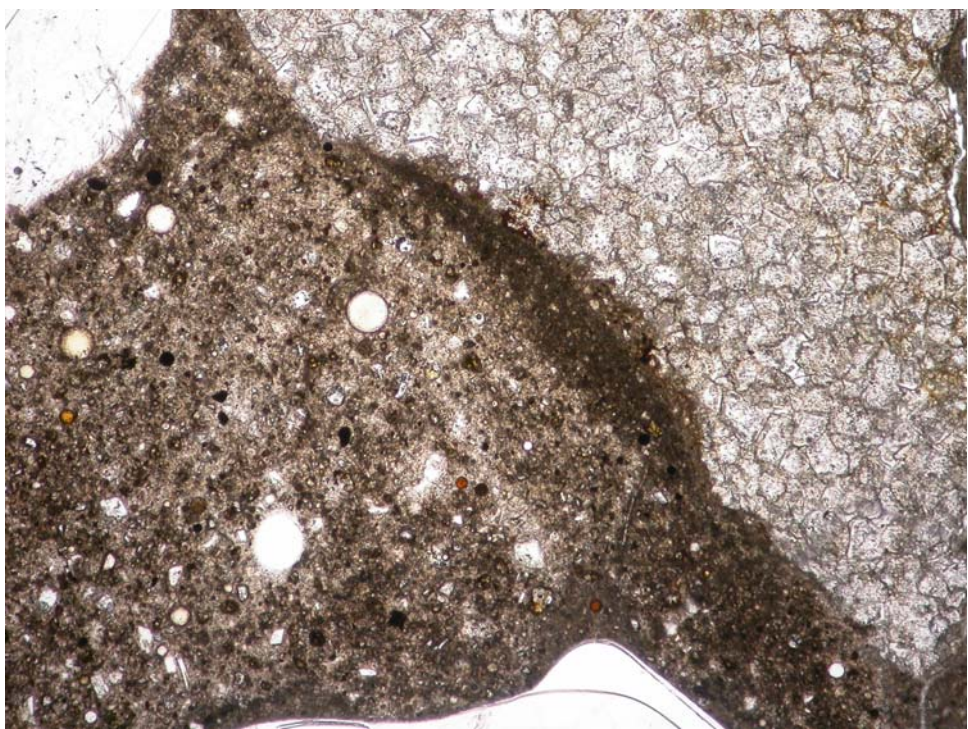


Photo #5: Thin section photomicrograph of paste inhomogeneities in Sample #1.
Planed-polarized light; Field Length = 2.8 mm

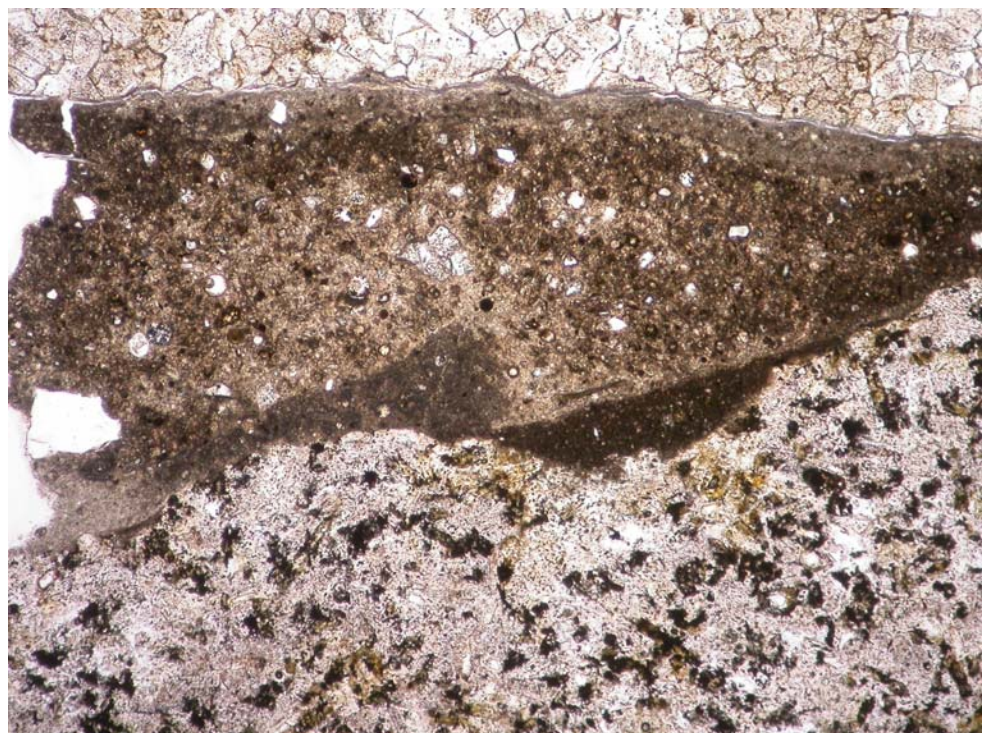


Photo #6: Thin section photomicrograph of paste inhomogeneities in Sample #2.
Planed-polarized light; Field Length = 2.8 mm

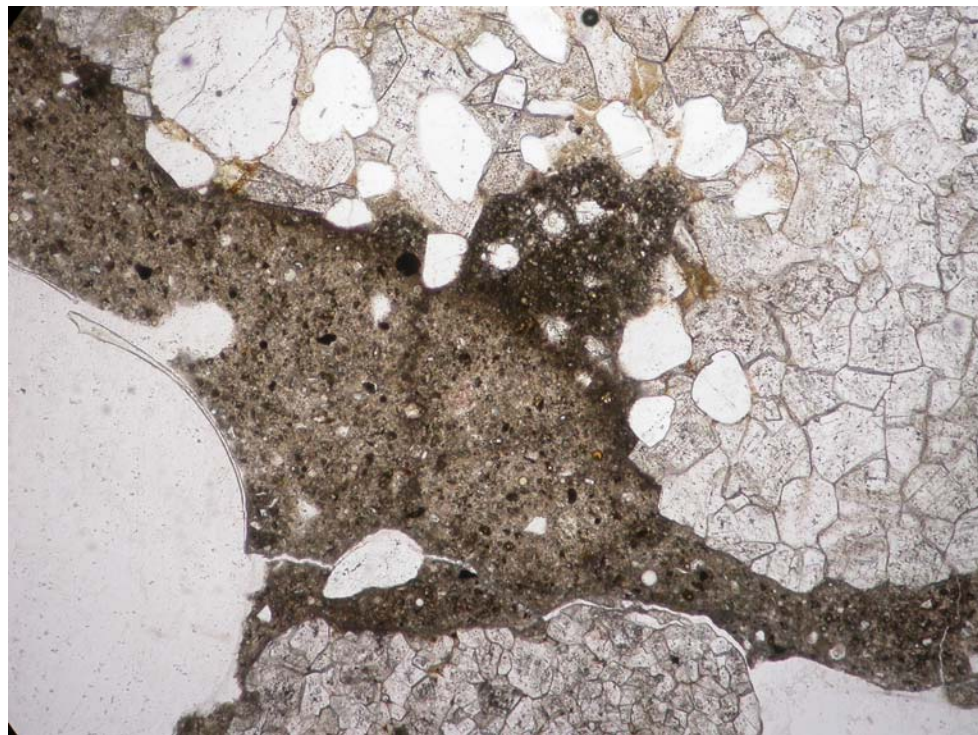


Photo #7: Thin section photomicrograph of paste inhomogeneities in Sample #3.
Planed-polarized light; Field Length = 2.8 mm



Photo #8: Thin section photomicrograph of paste inhomogeneities in Sample #4.
Planed-polarized light; Field Length = 2.8 mm



Photo #9: Thin section photomicrograph of the extensive cracking in Sample #1.
Plane-polarized light; Field Length = 2.8 mm

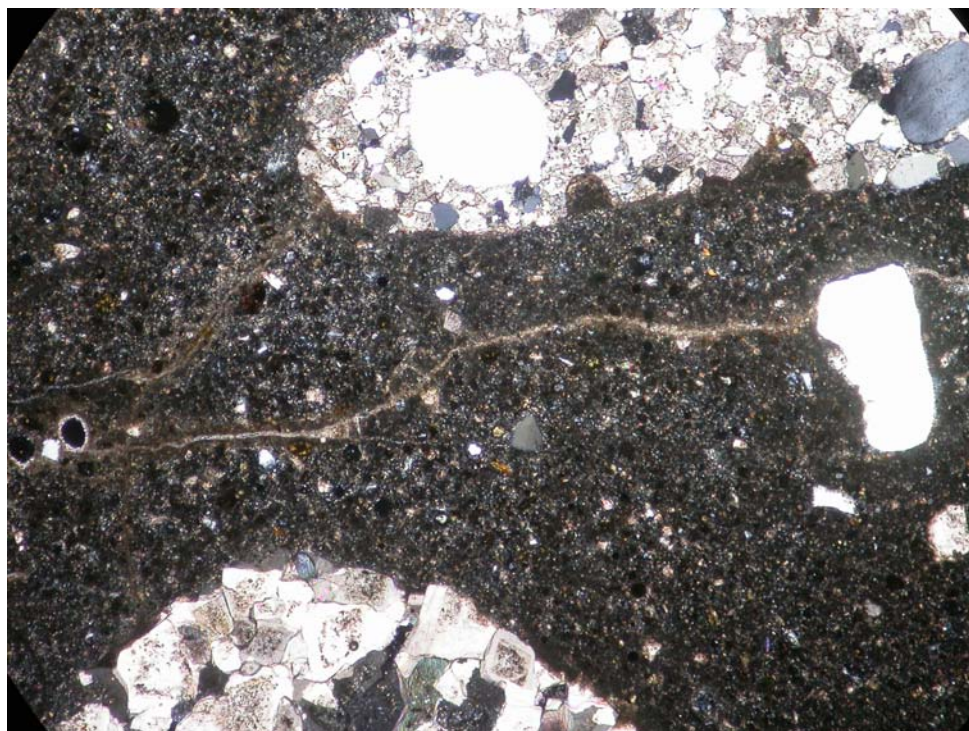


Photo #10: Thin section photomicrograph of a microcrack that has autogenously healed.
Cross-polarized light; Field Length = 2.8 mm



Photo #11: Photomicrograph of the air voids in Sample #1. Note the lack of entrained air in the paste regions. Scale: 1 division = 1 mm



Photo #12: Photomicrograph of the air voids in Sample #2. Note the lack of entrained air in the paste regions. Scale: 1 division = 1 mm



Photo #13: Photomicrograph of the air voids in Sample #3. Note the lack of entrained air in paste regions. Scale: 1 division = 1 mm



Photo #12: Photomicrograph of the air voids in Sample #4. Note the lack of entrained air in the paste regions. Scale: 1 division = 1 mm

APPENDIX D

PHOTOS OF CELL 64



FIGURE D-1: Tooled joint, Top: 9.21.06, Bottom: 8.11.08.



FIGURE D-2: Header/construction joint, Top: 9.21.06, Bottom: 8.11.08.



FIGURE D-3: Mix #2 surface raveling, Top: 01.04.06, Bottom: 8.11.08.



FIGURE D-4: Coterminous joint at Mixes #2 and #3, Top: 9.21.06, Bottom: 8.11.08.



FIGURE D-5: Header/construction joint, facing south, 8.11.08.



FIGURE D-6: Tooled joint, 4.02.09.



FIGURE D-7: Area of severe raveling in Mix 2, 4.02.09.



FIGURE D-8: Raveled surface material in Mix 2, 4.02.09.